A COMPUTATIONAL APPROACH TO TANGLES

by

NATHANIEL B. SCHIEBER

A THESIS

Presented to the Department of Mathematics
and the University of Oregon
in partial fulfillment of the requirements
for the degree of
Bachelors of Science

June 2018

THESIS ABSTRACT

Nathaniel B. Schieber

Bachelors of Science

Department of Mathematics

June 2018

Title: A Computational Approach to Tangles

This thesis has three main parts. In Chapters I–VI, we elaborate several constructions and results from knot theory. These are aimed at either beginning graduate students or advanced undergraduates and assume no prior experience with knots. However, a background in homology and module theory is recommended. In Chapters VII and VIII, we explain our technique in studying a particular tangle in the solid torus known as Krebes's tangle. Finally, in Chapter IX, we describe a process by which a small census of tangles of small complexity can be made.

ACKNOWLEDGEMENTS

This thesis would not have been possible without the support and guidance of Professor Robert Lipshitz. He introduced me not only to the specific problem but to the mathematics needed to study it. He has been a constant and reliable source of insight and encouragement. Neither the impact he has had on my mathematical career nor my gratitude for it could be overstated.

Therefore, I must also thank Professor Helen Wong from whom I first learned linear algebra and multivariable calculus at Carleton College. Three years after I left Carleton, she went above and beyond in helping me reapply to finish my undergraduate degree. When she heard that I would be attending the University of Oregon, she recommended that I take a course with Professor Lipshitz. I took his point-set course that fall and I have studied topology with him ever since.

Also at UO, I would like to thank professors Addington, Eischen, Gilkey, Lin, and Sinha for their commitment to helping me and my fellow students grow as a mathematicians. In particular, Professor Addington has assisted and advised me throughout my time at UO. I also wish to thank graduate students Mike Gartner and Andrew Wray for their friendship and for the mathematics they have shared with me.

Finally, I would like to acknowledge those who have helped me personally. I am indebted to no one more than my partner Daniela. I can not express the good that she represents in my life. She first encouraged me to return to academia and has put up with me ever since I did. I would also like to thank my parents Marc and Marsha and my sisters Hannah and Lily for their unconditional love and support. Others whom I would be remiss not to thank are Keith, Sean, Ariane, Lois, Alex, Fionna, Greg, James, Francois, Marcus, Kim, Andrew, Betsy, Fay, Ginger, Brigham, Tyler, Simon, Dan, Cameron, and Maile.

Thank you, all.

Nathaniel Bellamy Schieber
June 2018

For Daniela & Mayme

TABLE OF CONTENTS

CHAPTER I

KNOTS AND LINKS

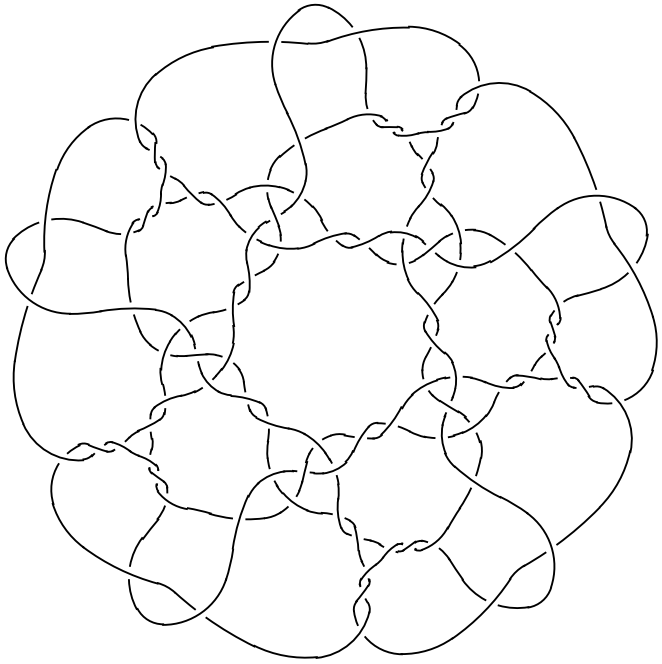

Figure 1.

Let us start by defining links. A ***link of n-components*** is the disjoint union of n smooth, simple closed curves in S^3. A link of one component is called a ***knot***. If each component of a link L is given an orientation, we say that L is an ***oriented link***. While we work with smooth links, one could also define a link to be a disjoint union of piecewise–linear, simple closed curves in S^3. A good reference for the piecewise–linear setting is [8].

We consider a few examples. First, a knot K is said to be an **unknot** if it bounds a smoothly embedded disc in S^3. For simplicity, one might visualize the unknot as a circle living within a plane in S^3. However, the particular embedding of an unknot might be much more complicated. For example, each of the knots shown in Figure 2 is an unknot. An n-component link L is said to be an **n-component unlink** if it is the disjoint union of n unknots which can be pairwise separated by open balls in S^3. Taken together, the unknots in Figure 2 form a 3-component unlink.

As a second example, consider Figure 3, which illustrates several stages of a particular embedding of a knot known as the figure eight knot. The red dot and dashes are meant to serve as markers to help visualize the embedding. The rightmost frame, shows the completed figure eight knot, with the arrow

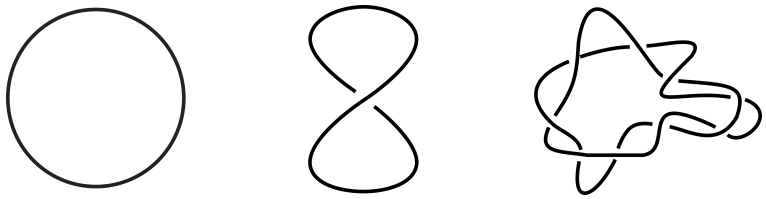

Figure 2.

representing the orientation inherited from the embedding. For many more examples of knots see [8], [9], and [12].

We would now like to define when two links are considered to be "the same." For this, we will need a more restrictive version of homotopy. Recall that a smooth homotopy H between two smooth maps $f, g : X \to Y$ is a smooth map $H : X \times I \to Y$ such that $H|_{X\times 0} = f$ and $H|_{X\times 1} = g$. If the maps f and g are both smooth embeddings and for each $t \in I$ the map $H|_{X\times t}$ is a smooth embedding, then H is called an **isotopy**. As a special case, suppose that $f, g : X \to X$ are diffeomorphisms. If f is the identity map, an isotopy $H : X \times I \to X$ between f and g such that $H|_{X\times t}$ is a diffeomorphism for each $t \in I$ is called an **ambient isotopy**.

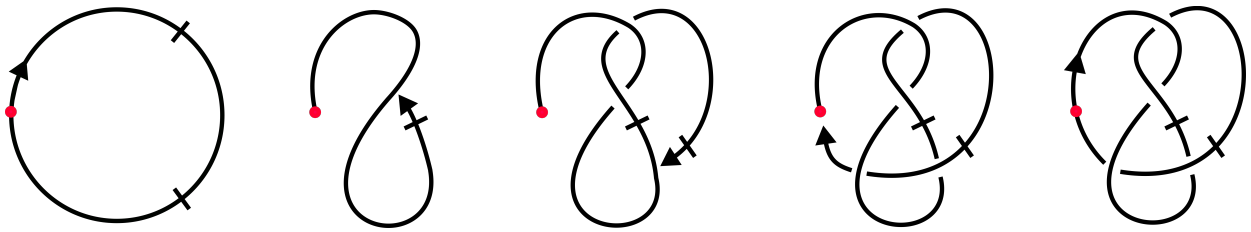

Figure 3.

Let L_1 and L_2 be two links in S^3. We say that L_1 and L_2 are **isotopic** if there exists an ambient isotopy $H : S^3 \times I \to S^3$ such that $H|_{S^3\times 1}(L_1) = L_2$. If L_1 and L_2 are oriented links, then the orientations of $H|_{S^3\times 1}(L_1)$ and L_2 must agree. This defines an equivalence relation on the collection of all links whose equivalence classes are called **isotopy classes** or **link types**. In general, we are interested in isotopy classes of links rather than in specific embeddings. Thus, when we write "let L be a link," we implicitly mean L to be a representative of an isotopy class.

We can also visualize an ambient isotopy between links. Let $H : S^3 \times I \to S^3$ be an ambient isotopy taking L_1 to L_2. Let $H_t = H|_{S^3\times t}$. As t travels from 0 to 1, the images of $H_t(L_1)$ form a movie showing L_1 smoothly deforming into L_2. Thus, we might intuitively think of two links as being isotopic if we can rearrange one into the other just as we might with our hands if our our links were tied from rope.

We also consider framed links. Let A be the annulus $S^1 \times [-1, 1]$. A **framed link** L is the image of a smooth embedding $\coprod_{i=1}^{n} A \to \mathbb{R}^3$. The image of $\coprod_{i=1}^{n} S^1 \times \{0\}$ in L is called the **underlying link** of L. An **oriented framed link** is a framed link where the underlying link is given an orientation. In this case, for each component of L, we consider both boundary components $S^1 \times \{-1\}$ and $S^1 \times \{1\}$ to be oriented in the same direction as $S^1 \times \{0\}$. Because A has two boundary components, so must each component of L. Hence, our definition does not allow for "Möbius" framed links, where the embedding incorporates a half–twist of A.

Two framed links L_1 and L_2 are **isotopic** if there exists an ambient isotopy $H : S^3 \times I \to S^3$ taking L_1 onto L_2. If L_1 and L_2 are oriented, then the orientations of $H|_{S^3 \times 1}(L_1)$ and L_2 must agree. As with unframed links, we generally consider isotopy classes of framed links.

A **framing** for a knot K is a choice of framed knot K' with underlying knot K. If $j \in \mathbb{Z}$, the **j-framing** for K corresponds to the unoriented framed knot K'_j with underlying knot K such that the linking number (defined in Chapter II) of K and the image of $S^1 \times \{1\}$ is equal to j. To compute the linking number, K and $S^1 \times \{1\}$ are oriented in the same direction. The two possible orientations define the same framing. Up to isotopy, framed knots are completely determined by the underlying knot and the framing number. Hence, to each knot K correspond $\mathbb{Z}$–many framed knots $\{K'_j\}_{j \in \mathbb{Z}}$. A **framing** for a link L is a choice of framing for each component.

Intuitively, we might think of a framed knot as a knot tied out of ribbon. Saying that a knot K is given the j-framing corresponds to tying K with a ribbon so that the ribbon twists around its central axis j times. For example, Figure 4 shows the unknot with two possible framings. Taken together, these form a framed link.

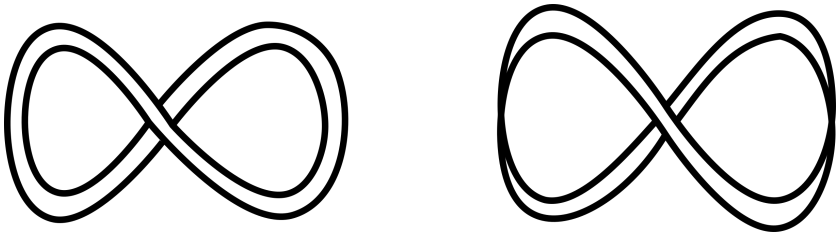

Figure 4.

Finally, as it will be useful in the next section, we note that we could also consider links to be disjoint unions of smooth, simple closed curves in $\mathbb{R}^3$. Shifting between the two settings causes little disturbance in our discussion for $S^3 = \mathbb{R}^3 \cup \{\infty\}$ and any link in S^3 is isotopic to a link disjoint from the

point ∞. Moreover, two links in $\mathbb{R}^3$ are isotopic if and only if they are isotopic as links in S^3. Thus, we consider links in whichever setting is more amenable to the task at hand.

CHAPTER II

LINK DIAGRAMS

We have now defined links—oriented and unoriented, framed and unframed—and when we consider two such links to be equivalent. However, these definitions are often difficult to apply. For example, writing down the explicit equations that describe an ambient isotopy would be quite complicated. To make this problem more tractable, we turn to link diagrams.

A **link diagram** D is the image of a smooth immersion $\coprod_{i=1}^{n} S^1 \to \mathbb{R}^2$ such that all self–intersections of D are transversal double points, carrying the following additional data. Each self–intersection is called a **crossing**. One of the two branches is distinguished as the **under crossing** and is represented by a broken line. The other branch is called the **over crossing**. Note that the crossing information does not depend on the immersion. In the special case that $n = 1$, D is called a **knot diagram**.

Two link diagrams D and D' are said to be **isotopic** if there exists an isotopy of the plane $H : \mathbb{R}^2 \times I \to \mathbb{R}^2$ such that $H|_{\mathbb{R}^2 \times 0} = \mathrm{id}_{\mathbb{R}^2}$, the identity map on $\mathbb{R}^2$, and $H|_{\mathbb{R}^2 \times 1}(D) = D'$. Note that for each $t \in I$, $H|_{\mathbb{R}^2 \times t}$ is a diffeomorphism. As with links, we consider link diagrams up to isotopy. If the image of each copy of S^1 is given an orientation, then D is called an **oriented link diagram**. We postpone our definition of framed linked diagrams until after Theorem 1.

Up to this point, most of the images of links found in this paper have, in fact, been link diagrams. Two non-examples are shown in Figure 5. The left–hand figure fails to be a link diagram as it has a point of triple intersection while the right–hand figure fails due a non-transversal point of intersection.

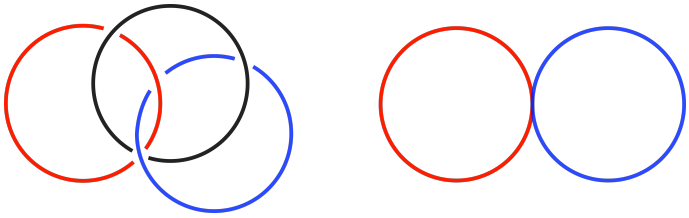

Figure 5.

We now consider the relation between links and link diagrams. We first show that every link diagram corresponds to a unique link type. Let D be a link diagram in the xy-plane in $\mathbb{R}^3$. In a small neighborhood of each crossing of D, smoothly push the over crossing off the xy-plane in the positive z direction and connect the two branches of the under crossing as shown in Figure 6. The result is a link L

in $\mathbb{R}^3$. The choices made in this process do affect the isotopy class of L and thus L is the unique link type to which D corresponds. In this case, we say that L **has link diagram** D or that L is **presented by** D.

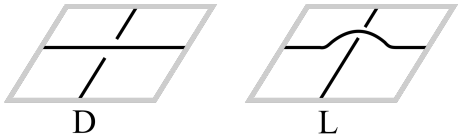

Figure 6.

We now show that every link can be presented by a link diagram. This requires substantially more work and we thus state it as the following theorem.

Theorem 1. *Every link $L \subset S^3$ can be presented by a link diagram $D \subset \mathbb{R}^2$.*

Proof: To begin, we show that if L is a link in $\mathbb{R}^3$, defined by an embedding f, then there exists a linear projection $\pi : \mathbb{R}^3 \to \mathbb{R}^2$ such that $\pi \circ f$ is an immersion. We adapt the proof of the Whitney Immersion Theorem found in [3].

Let $X = \coprod_{i=1}^{k} S^1$ and let $f : X \to \mathbb{R}^3$ be an embedding defining a link L. Let UTX be the unit tangent bundle of X and define the map $g : UTX \to S^2$ by $g(x,u) = df_x(u)/\left\|df_x(u)\right\|$. Note $df_x(u) \neq 0$ for all $(x,u) \in UTX$ as f is an immersion. Moreover, because $\dim UTX = 1$, every point in Im g is a critical value of g. By Sard's Theorem, Im g has measure 0 in S^2 and there exists a vector $a \in S^2 \setminus \text{Im } g$.

Define $H_a = \{b \in \mathbb{R}^3 : b \perp a\}$. That is, H_a is the orthogonal compliment in $\mathbb{R}^3$ to the line spanned by a. Let π be the orthogonal projection $\mathbb{R}^3 \to H_a$. We claim that $\pi \circ f$ is an immersion. For suppose that $d(\pi \circ f)_x(1) = 0$ for some $x \in X$. Then, since π is linear, the chain rule gives

$$d(\pi \circ f)_x(1) = \pi \circ df_x(1) = 0, \tag{2.1}$$

which implies that $df_x(1) = ca$ for some constant c. Hence,

$$\frac{df_x(1)}{\left\|df_x(1)\right\|} = \left(\frac{c}{\left\|df_x(1)\right\|}\right) a. \tag{2.2}$$

As both the left–hand vector and a are unit vectors, $c/\left\|df_x(1)\right\| = \pm 1$ and it follows that either $g(x,1) = a$ or $g(x,-1) = a$. In either case, this contradicts our choice of a and establishes our result.

We must now show that π can be chosen so that all points of self intersection in $\pi(L)$ are transversal. Let Δ represent the diagonal in $X \times X$ and define a map $\varphi = \varphi_2 \circ \varphi_1 : (X \times X) \setminus \Delta \to S^2$ by

$$(X \times X) \smallsetminus \Delta \xrightarrow{\varphi_1} \mathbb{R}^3 \smallsetminus 0 \xrightarrow{\varphi_2} S^2$$
$$(x, y) \longmapsto f(x) - f(y) \mapsto \tfrac{f(x)-f(y)}{\|f(x)-f(y)\|}.$$

By Sard's Theorem, the set of critical values of φ has measure 0. Thus, let $v \in S^2$ be a regular value of φ. Let $H_v = \{b \in \mathbb{R}^3 : b \perp v\}$ and let $\pi_v : \mathbb{R}^3 \to H_v$ be the orthogonal projection. Let $p \in \text{Im}\,(\pi_v \circ f)$ and assume that $\#(\pi_v \circ f)^{-1}(p) > 1$.

Suppose that $x, y \in (\pi_v \circ f)^{-1}(p)$ and $x \neq y$. It follows that $\varphi(x, y) = v$ for

$$(\pi_v \circ f)(x) = (\pi_v \circ f)(y) \;\; \Rightarrow \;\; \pi_v(f(x) - f(y)) = 0 \tag{2.3}$$

which implies that $f(x) - f(y)$ is a scalar multiple of v and hence, $\varphi(x, y) = \pm v$. Swapping the roles of x and y if necessary, we assume that $\varphi(x, y) = v$. We would like to show that $d(\pi_v \circ f)_x(1)$ and $d(\pi_v \circ f)_y(1)$ are linearly independent, for this will imply that the image of neighborhoods U_x of x and U_y of y under $\pi_v \circ f$ intersect transversally.

Assume to the contrary that $d(\pi_v \circ f)_x(1) = c_1 d(\pi_v \circ f)_y(1)$ for some nonzero constant c_1. By linearity and the chain rule, it follows that

$$\pi_v(df_x(1) - c_1 df_y(1)) = 0 \;\; \Rightarrow \;\; df_x(1) - df_y(c_1) = c_2 v \tag{2.4}$$

for some constant c_2. However, $d\varphi_{(x,y)} = d(\varphi_2)_{\varphi_1(x,y)} \circ d(\varphi_1)_{(x,y)}$ and we have

$$d\varphi_{(x,y)}(1, c_1) = d(\varphi_2)_{\varphi_1(x,y)}(df_x(1) - df_y(c_1)). \tag{2.5}$$

The fibers of φ_2 are lines through the origin and thus $\ker d(\varphi_2)_p = \{\alpha p : \alpha \in \mathbb{R}\}$ for any point $p \in \mathbb{R}^3$. Therefore, $\ker d(\varphi_2)_{\varphi_1(x,y)} = \{\alpha v : \alpha \in \mathbb{R}\}$. It now follows from Equation (2.5) that $d\varphi_{(x,y)}(1, c_1) = 0$ which contradicts our choice of v as a regular value of φ. Hence, there exists $v \in \mathbb{R}^3$ such that all points of self intersection in $\text{Im}\,(\pi_v \circ f)$ are transversal. Because both $\text{Im}\, g$ and the set of critical values of φ had measure 0 in S^2, we may choose a single vector $v \in S^2$ such that, under the projection $\pi_v : \mathbb{R}^3 \to \{b \in \mathbb{R}^3 : b \perp v\}$, the map $\pi_v \circ f$ is an immersion with all points of self–intersection are transversal.

Let $h = \pi_v \circ f$ and $D = h(X) \subset \mathbb{R}^2$. We can now show that D has at most finitely many points of self–intersection. Suppose to the contrary that D contains infinitely many points of self–intersection labelled $\{C_n\}_{n\in\mathbb{N}}$. Let $\{p_n\}$ and $\{q_n\}$ be sequences in X such that $p_n \neq q_n$ and $h(p_n) = h(q_n) = C_n$ for all

$n \in \mathbb{N}$. Because X is compact, we may pass to convergent subsequences $\{p_m\}$ and $\{q_m\}$. Let $p_m \to p$ and $q_m \to q$. By continuity, $h(p) = h(q)$.

We claim that $p \neq q$. Suppose to the contrary that $p = q$. Then, for large m, p_m and q_m fall in the same component of X. Since each point of self–intersection in D is transversal, the vectors $dh_{p_m}(1)$ and $dh_{q_m}(1)$ are linearly independent for all values of m. We may assume that $dh_{p_m}(1)$ and $dh_{q_m}(1)$ are orthogonal. Since h is smooth and $p = q$, both sequences $\{dh_{p_m}(1)\}$ and $\{dh_{q_m}(1)\}$ converge to $dh_p(1)$. However, this implies that $dh_p(1) = 0$, contradicting our construction of h as an immersion. Hence, $p \neq q$.

Put $C = h(p) = h(q)$. Since $p \neq q$, C is a point of self–intersection in D. By transversality, there exist neighborhoods U of p and V of q such that $h(U) \cap h(V) = C$. Thus, $U \cap \{p_m\} = \varnothing$ and $V \cap \{q_m\} = \varnothing$ and this contradicts the fact that $p_m \to p$ and $q_m \to q$. Therefore, D contains at most finitely points of self–intersection.

We now reduce each point of self intersection to a double point. Recall that immersions are a stable class of maps and that transversality is a stable property of maps. That is, if $F : X \times I \to \mathbb{R}^2$ is any smooth homotopy such that $F|_{X\times 0}$ is an immersion transversal to $Z \in \mathbb{R}^2$, then there exists $\epsilon > 0$ such that $F|_{X\times t}$ is an immersion transversal to Z for all $t \in [0, \epsilon]$.

Suppose that $p \in D$ such that $\#h^{-1}(p) = n$ for some $n > 2$. Since the self–intersection of D at p is transversal, there exists an open neighborhood U of p such that $h^{-1}(U)$ is the disjoint union of n open arcs in X. Let A be one of these arcs and let W be a closed neighborhood of $f(A)$ whose boundary intersects L in exactly two points, each time transversally, and such that $\partial W \cap f(A) = f(\partial A)$. Let u be a vector perpendicular to v and let ϵ_u be a smooth bump function such that $\epsilon_u(x) = 0$ for $x \in \partial A$, $\epsilon_u(x) > 0$ on $\mathrm{Int}A$, and such that $f(x) + \epsilon_u(x)tu \subset W$ for all $x \in f^{-1}(W)$ and all $t \in I$. Let $H : X \times I \to \mathbb{R}^3$ be an isotopy of L that fixes L on $\overline{\mathbb{R}^3 \setminus W}$ and such that $H(x, t) = f(x) + \epsilon_u(x)tu$ for all $x \in f^{-1}(W)$.

Define a smooth homotopy $F : X \times I \to \mathbb{R}^2$ by $F(x, t) = \pi_v \circ H(x, t)$. Then $F|_{X\times 0} = h = \pi_v \circ f$ and there exists $\epsilon > 0$ such that for all $t \in [0, \epsilon)$, $F|_{X\times t}$ is an immersion. Put $s = \epsilon/2$. Then $F|_{X\times s}$ is a smooth immersion such that $\#{F|_{X\times s}}^{-1}(p) = n - 1$. Moreover, because H was an isotopy, we did not change the isotopy class of L. As there are only finitely many points of self–intersection, we may repeat this process until all points of self–intersection are transversal double points. This completes the proof. □

We will have a similar result for framed links and framed link diagrams. However, to consider framed link diagrams, we must define the blackboard framing. Let D be a link diagram defined by an immersion $f : \coprod_{i=1}^{n} S_i^1 \to \mathbb{R}^2$. Let $\sigma_i, \mu_i : f(S_i^1) \to \mathbb{R}^2$ be the two possible smooth normal vector fields

on $f(S_i^1)$ of uniform length ϵ_i for $i = 1, 2, \ldots, n$. Together, these define an immersed annulus $A_i \subset \mathbb{R}^2$ which we parameterize by $\varphi_i : S^1 \times [-1, 1] \to \mathbb{R}^2$ such that $\varphi_i(S^1 \times \{0\}) = f(S_i^1)$. Intuitively, each A_i is a thickened ribbon, lying flat in the plane and tracing out $f(S_i^1)$. Let $\varphi = \coprod_{i=1}^n \varphi_i : \coprod_{i=1}^n S_i^1 \times [-1, 1] \to \mathbb{R}^2$. Since all points of self–intersection are transversal in D, we may shrink ϵ_i if necessary, for $i = 1, 2, \ldots, n$, such that φ fails to be injective only within a neighborhood of each crossing.

Let $D_{\text{fr}} = \text{Im } \varphi$ together with the crossing information inherited from D. We call any diagram D_{fr} obtained from D in this manner, D with the **blackboard framing**. In D_{fr}, we record the crossing information as shown in the left–hand diagram in Figure 4. A **framed link diagram** is a link diagram D that has been given the blackboard framing. Note that we do not consider the right–hand diagram in Figure 4 to be a framed link diagram as the annulus does not lay flat in the plane.

If D_{fr} and D'_{fr} both represent D with the blackboard framing, they differ at most by a choice of values ϵ_i and parameterizations φ_i. Modulo these inconsequential differences, the blackboard framing of a link diagram is unique. Thus, when we draw framed link diagrams we simply draw link diagrams and implicitly assume the blackboard framing. We have the following lemma.

Lemma 1. *Every framed link diagram corresponds to a unique framed link and every framed link can be represented by a framed link diagram.*

Proof: To see that every framed link diagram corresponds to a unique framed link, we follow the same procedure as with unframed link diagrams, smoothly pushing the over crossing off of the plane. For the second statement, recall that framed links are determined, up to isotopy, by the isotopy class of their underlying link and the framing number. Since we have already shown that all links can be represented by link diagrams, it suffices to show that all framings for a link L can be presented as the blackboard framing of some link diagram presenting L. This will be immediate after Theorem 2. □

Let us focus on unoriented, unframed links. We note that the correspondence between links and link diagrams is not one-to-one. Figure 2, for example, shows three knot diagrams all corresponding to the unknot. Nevertheless, we do have an algorithmic means of relating link diagrams via local transformations of three possible forms. These are the **Reidemeister moves**, shown in Figure 7. Each describes the relation between two link diagrams which are identical outside of a small neighborhood, in which they differ as shown.

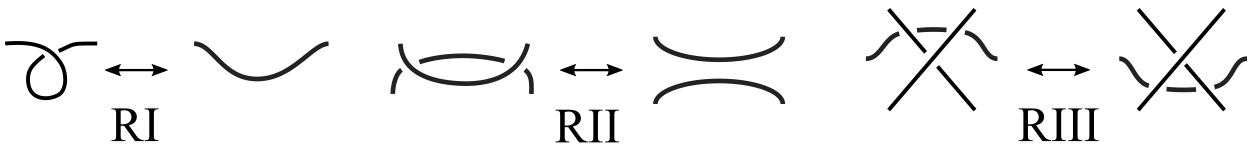

Figure 7.

Although the statement of the following theorem seems straightforward, its proof is quite complicated. A translation of Reidemeister's original paper can be found in [11] and accessible outlines of his proof can be found in either [6] or [10].

Theorem 2. *Two unoriented, unframed links L and L' are isotopic if and only if they correspond to unoriented link diagrams D and D' which are related, up to isotopy, by a finite sequence of the moves RI, RII, and $RIII$.*

There are analogous theorems in the contexts of oriented and framed links. These are also found in [10]. Their statements are the same but the list of Reidemeister moves varies in each case. For oriented link diagrams, we consider the **oriented Reidemeister moves**, denoted $\overrightarrow{RI}, \overrightarrow{RII}$, and $\overrightarrow{RIII}$, which are shown in Figure 8.

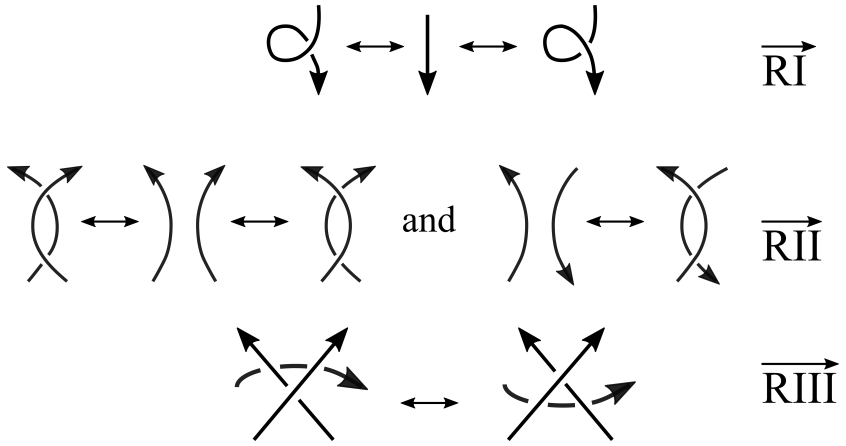

Figure 8.

For framed link diagrams, we still use the RII and $RIII$ moves from Figure 7. However, performing the RI move either adds or removes a "twist" in the framing, changing the framing number by ± 1. As a result, when considering Reidemeister moves for framed tangle diagrams, we replace the RI move by the framed RI move shown in Figure 9 so as not to alter the framing.

Yet, it is this effect of the unframed RI move on the framing that allows us to complete the proof of Lemma 1. If a framed link L_{fr} has underlying link L presented by a diagram D, we may alter D by a sequence of RI moves to form a new diagram D' such that, when given the blackboard framing, D' presents L_{fr}. Thus, all framings for a given link L can be presented as the blackboard framing.

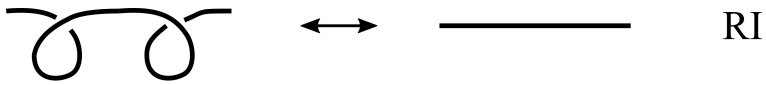

Figure 9.

To end this section, we introduce two properties of oriented link diagrams that will prove useful. Necessary to each will be the following definition. Let D be an oriented link diagram with at least one crossing. Locally, each crossing of D takes one of the two forms shown in Figure 10, which we define to be either a **positive crossing** or a **negative crossing**.

After labelling each crossing of D, with either a $+1$ or a -1, the sum over all crossings of these labels is known as the **writhe** of the diagram D and is denoted $\omega(D)$.

Now let L be a link of at least two components and let D be a link diagram of L. Label two of the components L_1 and L_2 respectively. Let S be the set of crossings of D that involve both L_1 and L_2. We define the **linking number** of L_1 and L_2, denoted $lk(L_1, L_2)$, to be half the sum of the signs of the crossings in S.

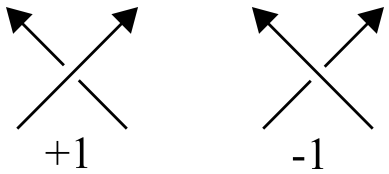

Figure 10.

Lemma 2. *Let L be a link of at least two components and D a link diagram presenting L. Let L_1 and L_2 be two components of L. Then $lk(L_1, L_2)$ is an isotopy invariant of L.*

Proof: We show that $lk(L_1, L_2)$ is unchanged when D is altered by the Reidemeister moves. That $lk(L_1, L_2)$ is invariant under the $\overrightarrow{RI}$ move is immediate since the $\overrightarrow{RI}$ move pertains to one component of the link diagram crossing itself. We see that the move $\overrightarrow{RIII}$ leaves the linking number unchanged as it preserves both the number of crossings as well as their signs. Finally, the linking number is invariant

under the $\overrightarrow{RII}$ move because this move either adds or removes a pair of crossings of opposite sign. It now follows from Theorem 2 that $lk(L_1, L_2)$ is an isotopy invariant of L. $\square$

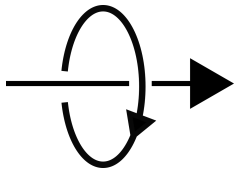

Figure 11.

The linking number can also be defined in terms of homology. Consider an oriented link $L \subset S^3$ with two components labelled L_1 and L_2. Using the Mayer–Vietoris sequence, it is not hard to show that $H_1(S^3 \setminus L_2) \cong \mathbb{Z}$. We postpone the proof until Chapter V. The isomorphism $\varphi : H_1(S^3 \setminus L_2) \to \mathbb{Z}$ is determined by the orientation of L_2 via the right–hand rule, shown in Figure 11. That is, the closed curve shown represents the generator of $H_1(S^3 \setminus L_2)$ that maps to $+1$ in $\mathbb{Z}$. We can now define the linking number by $lk(L_1, L_2) = \varphi([L_1])$.

Lemma 3. *These two definitions of linking number agree.*

Proof: Let D be a link diagram that presents L. Let S be the set of crossings in D that involve both L_1 and L_2. Within a neighborhood of each crossing of S, we may alter D by changing positive crossings to negative crossings or vice versa, one–by–one, until we attain a new diagram D', in which L_1 passes under L_2 each time they meet. Let S' be the collection of these crossings.

Let L' be the link in S^3 corresponding to D' and let π be the projection that defines D'. As L_1 always passes under L_2, we may assume, after an isotopy if necessary, that L_1 and L_2 are separated in S^3 by a plane P, perpendicular to the direction of the projection π. It follows that L_1 is null–homotopic in $S^3 \setminus L_2$ and thus $\varphi([L_1]) = 0$. Moreover, we may isotope L' again, translating L_1 in a direction parallel to P far enough such that $\pi(L')$ now contains no crossings involving both L_1 and L_2. As the linking number is an isotopy invariant, we have that $\sum_{s \in S'} \operatorname{sgn}(s) = 0$ and we compute $\operatorname{lk}(L_1, L_2) = 0$ in L' using both definitions.

Let us consider the effect that altering a single crossing has on either computation. In the diagrammatic definition we have that $\operatorname{lk}(L_1, L_2) = (1/2) \sum_{s \in S} \operatorname{sgn}(s)$. Replacing a positive crossing with a negative, decreases the sum by 2 and thus decreases $\operatorname{lk}(L_1, L_2)$ by 1. Conversely, replacing a negative crossing with a positive crossing increases $\operatorname{lk}(L_1, L_2)$ by 1.

The effect on homology requires more geometry. Assuming that the direction of the projection π is directly into the page, replacing a positive crossing in D with a negative crossing corresponds to a local transformation of L as shown in Figure 12. L_1 is replaced by L_1' and they are identical outside of the ball shown. Let $[\sigma]$ be the generator of $H_1(S^3 \setminus L_2)$ shown in Figure 11. Suppose that $[L_1] = k[\sigma]$, which

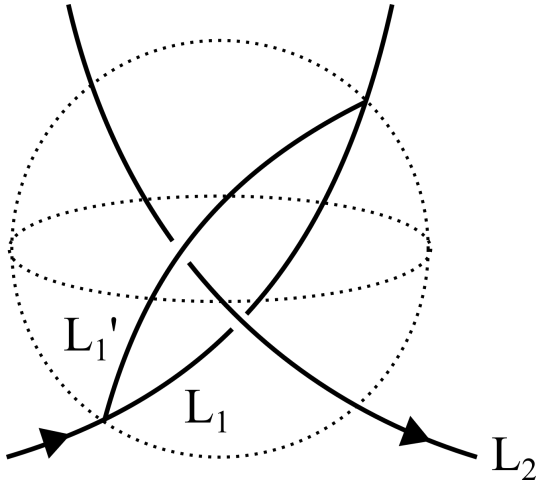

Figure 12.

implies that $\varphi([L_1]) = k$. We see that L_1 and L_1' bound an annulus that deformation retracts onto a curve homotopic to either $\pm\sigma$. More specifically, we see that

$$[L_1] - [L_1'] = k[\sigma] - [L_1'] = [\sigma] \quad \Rightarrow \quad [L_1'] = (k-1)[\sigma]. \tag{2.6}$$

That is, $\varphi([L_1']) = k - 1$. Therefore changing a positive crossing to a negative crossings decreases $\varphi([L_1])$ by 1. Conversely, changing a negative crossing to a positive crossing corresponds to replacing L_1' by L_1. Supposing that $[L_1'] = k[\sigma]$, we find $[L_1'] - [L_1] = -[\sigma]$ and thus $[L_1] = (k+1)[\sigma]$. Hence, changing a negative crossing to a positive crossing increases $\varphi([L_1'])$ by 1.

Combining our results, we see that altering a crossing in D has the same affect on the linking number as computed using either definition. As the same sequence of changes brought both computations to 0, our definitions must have agreed on L. As L was arbitrary, they agree in general. $\square$

CHAPTER III

THE KAUFFMAN BRACKET AND JONES POLYNOMIAL

To study link diagrams, we now consider a map known as the Kauffman Bracket, first discovered by Kauffman in [5]. Our construction follows that in [8]. The **Kauffman Bracket** is a function from unoriented link diagrams to the polynomial ring $\mathbb{Z}[A, A^{-1}]$ where A is a formal variable. It sends a diagram D to $\langle D\rangle \in \mathbb{Z}[A, A^{-1}]$ and it is characterized by the three relations shown in Figure 13.

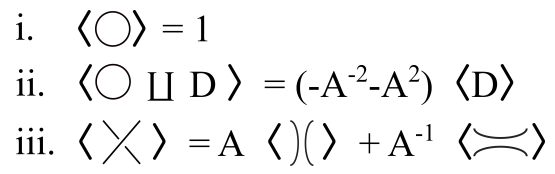

Figure 13.

For clarity, let D_0 represent any diagram of the unknot with no crossings. We remark that relation **i.** says that $\langle D_0\rangle = 1$. Relation **ii.** says that if $D' = D_0 \amalg D$ for some diagram D, then $\langle D'\rangle = (-A^{-2} - A^2)\langle D\rangle$. The relation **iii.** is known as the **Kauffman bracket skein relation** and gives the relation between three link diagrams that are identical except within a neighborhood of a crossing where they differ as indicated.

Using these relations, the Kauffman bracket $\langle D\rangle$ of a diagram D can be computed by expanding all crossings of D according to the skein relation. If D has n crossings, then the result of this expansion is the disjoint union of 2^n copies of D_0. Thus, using relation **iii.** we have that $\langle D\rangle = \sum_{i=1}^{2n} p_i\langle D_0\rangle$ where the coefficients p_i are polynomials in $\mathbb{Z}[A, A^{-1}]$. This result did require a choice of order in which to expand the crossings. However, it is not hard to show, by transposing adjacent crossings in some order, that this choice is immaterial. It now follows from the relations **i.** and **ii.** that $\langle D\rangle$ is a well–defined polynomial in $\mathbb{Z}[A, A^{-1}]$. The empty diagram has bracket $\langle\ \rangle = (-A^{-2} - A^2)^{-1}$ for

$$1 = \langle D_0\rangle = \langle D_0 \amalg \quad \rangle = (-A^{-2} - A^2)\langle\ \rangle. \tag{3.1}$$

The following lemma describes the effect of the unoriented Reidemeister moves on $\langle D\rangle$.

Lemma 4. *Let D be an unoriented link diagram.*

- **a.** *If D is changed by an RI move then $\langle D\rangle$ changes as shown in Figure 14.*
- **b.** *If D is changed by an RII or RIII move, then $\langle D\rangle$ does not change.*

Figure 14.

We leave the proof as an exercise. Importantly, we note that part **a.** implies that the Kauffman bracket is an invariant of framed links. Moreover, when used in conjunction with writhe, the Kauffman bracket gives an invariant of unframed, oriented links. This is the Jones polynomial, defined as follows.

Let D be an oriented link diagram. The writhe $\omega(D)$ is invariant under the moves $\overrightarrow{RII}$ and $\overrightarrow{RIII}$ because the move $\overrightarrow{RII}$ either adds or removes a pair of crossings of opposite sign and $\overrightarrow{RIII}$ leaves the number of crossings and their signs unchanged. However, under the $\overrightarrow{RI}$ move, $\omega(D)$ changes by either $+1$ or -1. We have thus been lead to the following result.

Theorem 3. *Let D be an oriented link diagram corresponding to an oriented link L. Then the expression*

$$(-A)^{-3\omega(D)}\langle D\rangle \tag{3.2}$$

is an invariant of the oriented link L.

Proof: That the expression (3.2) is unchanged by the moves $\overrightarrow{RII}$ and $\overrightarrow{RIII}$ follows from the fact that both $\omega(D)$ and $\langle D\rangle$ are invariant under these moves, $\langle D\rangle$ being invariant under the corresponding moves RII and $RIII$. Moreover, (3.2) is unchanged by the $\overrightarrow{RI}$ move by the above remarks on $\omega(D)$ and part **a.** of Lemma 4. Hence, (3.2) is invariant under the moves $\overrightarrow{RI}, \overrightarrow{RII}$, and $\overrightarrow{RIII}$ and is therefore an invariant of oriented links. □

The **Jones polynomial** $V(L)$ of an oriented link L is then defined to be the Laurent polynomial in $\mathbb{Z}[t^{1/2}, t^{-1/2}]$ defined by

$$V(L) = \Big((-A)^{-3\omega(D)}\langle D\rangle\Big)_{t^{1/2}=A^{-2}}. \tag{3.3}$$

Here, $t^{1/2}$ is just a formal variable whose square is t. From this definition, it is immediate that $V(unknot) = 1$. However, classifying knots with Jones polynomial 1 remains an open question. While there are nontrivial links with trivial Jones polynomial, as shown in [13], the following conjecture has remained open since it was first proposed in the 1980's.

Conjecture 1. *The unknot is the unique knot with Jones polynomial* 1*.*

Though we will not make heavy use of the Jones polynomial moving forward, we do use a similar construction to derive an invariant of tangles.

CHAPTER IV

THE ALEXANDER POLYNOMIAL

The Alexander polynomial was the first knot polynomial discovered. However, we will need some preliminary results from algebra and algebraic topology in order to make sense of its definition. Good references are [2] and [4] respectively.

Let R be a commutative ring with unity $\mathbb{1}_R$. An **R-module** is an abelian group M together with a bilinear map $R \times M \to M$ written $(r, m) \mapsto rm$ such that for all $r, s \in R$ and $m \in M$,

$$r(sm) = (rs)m \quad \text{and} \quad \mathbb{1}_R m = m. \tag{4.1}$$

Note that a vector space is a module over a field. Hence, module theory serves as a generalization of linear algebra. For example, if M is an R-module then M^*, the **dual module** to M, is the module of maps $M \to R$. That is, $M^* = \mathrm{Hom}\,(M, R)$.

An R-module is called **free** if it is isomorphic to a direct sum of copies of R. If M is an R-module a **presentation** of M is an exact sequence

$$F_1 \xrightarrow{f} F_0 \to M \to 0 \tag{4.2}$$

where F_0 and F_1 are free R-modules. If F_1 and F_0 are finitely generated, we may choose bases for each, and represent the map f by a matrix A, called a **presentation matrix** for M. We will work only with modules that admit presentations of this form.

Let M and N be R-modules. The **tensor product** of M and N over R, denoted $M \otimes_R N$ is defined as follows. Let S be the free R-module of all formal symbols $m \otimes n$ for $m \in M$ and $n \in N$. Then $M \otimes_R N$ is the quotient of S by all relations of the form

$$(am + a'm') \otimes (bn + b'n') = ab(m \otimes n) + a'b(m' \otimes n) + ab'(m \otimes n') + a'b'(m' \otimes n') \tag{4.3}$$

where $a, b \in R$. When the ring R is clear from the context, we write the tensor product simply as $M \otimes N$. A **commutative algebra** over R is a commutative ring S together with a ring homomorphism $R \to S$.

We combine these definitions. If M in an R-module, the **tensor algebra** of M is the graded, non-commutative algebra

$$T_R(M) = R \oplus M \oplus (M \otimes M) \oplus (M \otimes M \otimes M) \oplus \cdots \tag{4.4}$$

where multiplication is defined by concatenation of tensors. That is, $(x_1 \otimes \cdots \otimes x_m)(y_1 \otimes \cdots \otimes y_n) = x_1 \otimes \cdots \otimes x_m \otimes y_1 \otimes \cdots \otimes y_n$. The term "graded" refers to the fact that we may decompose $T_R(M)$ into subalgebras $T_R^j(M)$ which consist of all j-fold tensor products.

The **exterior algebra** of M over R is the graded algebra $\wedge_R M$ obtained from $T_R(M)$ by imposing skew-commutativity. That is, $\wedge_R M$ is the quotient of $T_R(M)$ by the relations $x_1 \otimes x_2 = -x_2 \otimes x_1$. When working in $\wedge_R M$ we replace the tensor product $\otimes$ with the wedge product $\wedge$. As with the tensor algebra, we may decompose $\wedge_R M$ into subalgebras $\wedge_R^j M$ which consist of all j-fold wedge products.

Suppose that $\varphi : F \to G$ is a map between free R-modules. Then φ induces a map $\wedge\varphi : \wedge F \to \wedge G$ by setting $\wedge\varphi(x_1 \wedge \cdots \wedge x_n) = \varphi(x_1) \wedge \cdots \wedge \varphi(x_n)$ and extending linearly. From this definition, we see that, more specifically, φ induces a maps $\wedge^j\varphi : \wedge^j F \to \wedge^j G$ for each $j = 0, 1, 2, \ldots$.

Furthermore, the map $\wedge^j\varphi : \wedge^j F \to \wedge^j G$ induces a map

$$\widetilde{\varphi}^j : \wedge^j F \otimes \wedge^j G^* \to R \qquad \text{given by} \tag{4.5}$$

$$(x_1 \wedge \cdots \wedge x_j) \otimes (y_1^* \wedge \cdots \wedge y_j^*) \mapsto \sum_\sigma (-1)^{\operatorname{sgn}(\sigma)} y_{\sigma(1)}(x_1) \cdots y_{\sigma(j)}(x_j) \tag{4.6}$$

where σ represents a permutation on j variables and the sum is taken over all permutations. Denote the image of $\widetilde{\varphi}^j$ by $I_j\varphi$. If we chooses bases for F and G, then φ can be expressed as a matrix and $I_j\varphi$ is generated by the minors (ie. determinants of submatrices) of size j of that matrix. We use the convention that the determinant of a 0×0 matrix is 1. Hence, $I_0\varphi = R$. More generally, we set $I_j\varphi = R$ for $j < 0$. We have thus been lead to the following lemma, whose proof can be found in [2].

Lemma 5. ***(Fitting's Lemma)*** *Let M be a finitely generated module over a ring R, and let $F \xrightarrow{\phi} G \to M \to 0$ and $F' \xrightarrow{\phi'} G' \to M \to 0$ be two presentations, with G and G' finitely generated free modules of ranks r and r'. For each number i with $0 \leq i < \infty$, we have $I_{r-i}(\varphi) = I_{r'-i}(\varphi')$, and we define the **$i$th Fitting invariant** or **ith Fitting ideal** of M to be the ideal*

$$\operatorname{Fitt}_i(M) = I_{r-i}\varphi \subset R. \tag{4.7}$$

That is, the Fitting ideals of a module depend neither on the presentation nor the presentation matrix of that module. Fitting ideals are thus a module invariant.

We now return to topology and restrict our attention to knots. Let K be a knot. We show that $H_1(S^3 \setminus K) \cong \mathbb{Z}$ using the Mayer–Vietoris sequence. Let $T \subset S^3$ be an embedded solid torus $D^2 \times S^1$ such that K is the image of $\{(0,0)\} \times S^1$ under the embedding. Let $A = \text{Int}(T)$ and let B be the compliment of $f(C)$ in S^3 where C is the subspace of $D^2 \times S^1$ defined by

$$C = \left\{((x,y),s) : x^2 + y^2 \leq \frac{1}{2}\right\}. \tag{4.8}$$

That is, $B = S^3 \setminus f(C)$. A cross section of the A is shown in Figure 15 where A is shown in blue and B corresponds to the dotted region.

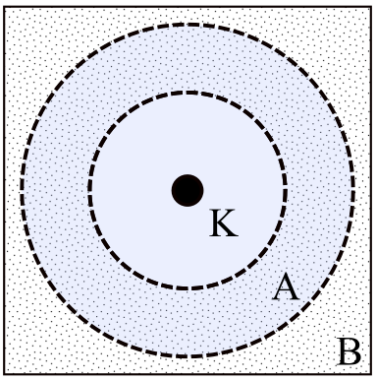

Figure 15.

We have defined our spaces so that $A \cup B = S^3$, A is homotopy equivalent to K, and B is homotopy equivalent to $S^3 \setminus K$. It follows that $H_1(A) \cong \mathbb{Z}$. Moreover, $A \cap B$ is homotopy equivalent to a torus and thus $H_1(A \cap B) \cong \mathbb{Z} \oplus \mathbb{Z}$. Because S^3 has trivial homology in dimensions 1 and 2, the Mayer–Vietoris sequence corresponding to the triple A, B and $A \cup B$ contains the segment

$$\cdots \longrightarrow H_2(S^3) \longrightarrow H_1(T^2) \longrightarrow H_1(K) \oplus H_1(S^3 \setminus K) \longrightarrow H_1(S^3) \longrightarrow \cdots$$

$$\cdots \longrightarrow 0 \longrightarrow \mathbb{Z} \oplus \mathbb{Z} \longrightarrow \mathbb{Z} \oplus H_1(S^3 \setminus K) \longrightarrow 0 \longrightarrow \cdots .$$

By exactness, we have that $\mathbb{Z} \oplus \mathbb{Z} \cong \mathbb{Z} \oplus H_1(S^3 \setminus K)$ and therefore $H_1(S^3 \setminus K) \cong \mathbb{Z}$, as claimed.

We can now use this result to determine a specific covering space of $S^3 \setminus K$ known as the infinite cyclic cover. The **knot group** of a knot K is then defined to be $\pi_1(S^3 \setminus K)$, the fundamental group of the compliment of K in S^3. If two knots K and K' are isotopic then the isotopy between them, extends to

an isotopy of S^3. This defines an isotopy between $S^3 \setminus K$ and $S^3 \setminus K'$, which induces an isomorphism between their fundamental groups. The knot group is thus a knot invariant. Much more on the knot group and its various properties can be found in [12].

Let G be the knot group of a knot K. By the Hurewicz Theorem, $H_1(S^3 \setminus K)$ is isomorphic to the abelianization of G. Hence, $H_1(S^3 \setminus K) \cong G/[G,G]$ where $[G,G]$ denotes the commutator subgroup. Let X^∞ be the covering space of X corresponding to $[G,G]$. Because $[G,G]$ is a normal subgroup of G, X^∞ is a normal covering space and thus its group of deck transformations F is isomorphic to $G/[G,G] \cong \mathbb{Z}$. For this reason, we call X^∞ the **infinite cyclic cover** of $S^3 \setminus K$.

Let t be a translation that generates F. Then $H_1(X^\infty)$ is a $\mathbb{Z}[t,t^{-1}]$ module by the following lemma.

Lemma 6. *If X is a topological space with a $\mathbb{Z}$ action generated by $t : X \to X$, then $H_i(X)$ is a $\mathbb{Z}[t,t^{-1}]$-module for $i = 0, 1, 2, \ldots$.*

Proof: Define the multiplication map $\mathbb{Z}[t,t^{-1}] \times H_i(X) \to H_i(X)$ by

$$(at^n, [\sigma]) \mapsto a[t^n \circ \sigma], \tag{4.9}$$

where $t^n \circ \sigma$ is the map σ composed with the n-fold composition of t with itself, and extending bilinearly. Checking that this gives $H_i(X)$ the structure of a $\mathbb{Z}[t,t^{-1}]$-module is straightforward. □

The **jth Alexander polynomial** of K is

$$\Delta_K^j(t) \doteq p_j(t) \tag{4.10}$$

where $p_j(t) \in \mathbb{Z}[t,t^{-1}]$ is a generator of the smallest principal ideal containing $\text{Fitt}_j(H_1(X^\infty))$. Here, the symbol $\doteq$ means equal up to multiplication by a unit, which in $\mathbb{Z}[t,t^{-1}]$ is a monomial of the form $\pm t^b$ for any integer b. In general, the first Alexander polynomial of a knot K is simply called the **Alexander polynomial** of K and is denoted $\Delta_K(t)$. Because fitting ideals are a module invariant and because $H_1(X^\infty)$ is an invariant of knots, we have proved the following theorem.

Theorem 4. *The Alexander polynomial is a knot invariant.*

We note that $\Delta_{unknot}(t) \doteq 1$. However, there are knots K, not equivalent to the unknot, such that $\Delta_K(t) \doteq 1$. The Kinoshita-Terasaka knot, shown in Figure 16 is one such example. Hence, the Alexander polynomial is not a complete knot invariant. Moreover, there are pairs of knots K and K' such

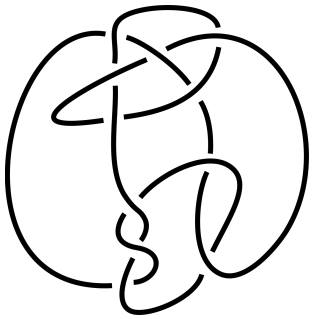

Figure 16.

that $\Delta_K(t) \neq \Delta_{K'}(t)$ yet $\Delta_K^j(t) \doteq \Delta_{K'}^j(t)$ for some $j > 1$. Note that we have defined the Alexander polynomial only for knots and not for links in general. While there is an extension of the Alexander poylnomial to links, known as the **multivariable Alexander polynomial**, we will not need it here and so do not develop it.

CHAPTER V

TANGLES

As a generalization of links, we now consider tangles. Let $B = B^3$ be the standard 3-ball in S^3 and let $S^2 = \partial B$. A **tangle** T is a compact 1-manifold with boundary, embedded in B such that the boundary of T lies in S^2 with $T \pitchfork S^2$. More specifically, we require that $\partial T \subset W \setminus \{(\pm 1, 0, 0)\}$ where $W = (S^2 \cap xy\text{-plane})$. Though one can certainly consider tangles without this last requirement, we use it as a means to enrich our discussion.

Let T be a tangle in B and let $\mathbb{H}^+$ and $\mathbb{H}^-$ be the open upper and lower half–planes of the xy-plane. Let $W^\pm = W \cap H^\pm$. Call those boundary points of T that fall in W^+ **inputs** and those that fall in W^- **outputs**. Starting from $(-1, 0, 0)$ and traveling in the positive x-direction along W^+, the inputs of T inherit an ordering and we label them $v_1, \ldots, v_m$ accordingly. Similarly, starting from $(-1, 0, 0)$ and traveling in the positive x-direction along W^-, the outputs of T inherit an ordering and we label them $w_1, \ldots, w_n$. Note that the collection of all inputs and outputs also inherits a cyclic ordering.

If each component of a tangle T is given an orientation, T is called an **oriented tangle**. We say that a tangle T is an **n-component untangle** if T has n inputs, n outputs, and is isotopic to the tangle which is given by the n line segments $\{\overline{v_i w_i}\}_{i=1}^n$.

Our definition of framed tangles requires more care. In short, a **framed tangle** is a tangle T where each component is given a framing. For the closed components of T, this agrees with our definition of a framing for a knot in Chapter I. However, we must define what we mean by a framing for those components of T with boundary. Let $C \subset T$ be one such component and let I be the unit interval $[0, 1]$. A **framing** for C is a choice of embedding $I \times I \to B$ such that $\{1/2\} \times I = C$, $(I \times I) \cap (W^+ \cup W^-) = I \times \{0, 1\}$, and $I \times I \pitchfork W$. The **j-framing** for C is an embedding of $I \times I$ which twists j times around its central axis. Of course, we require that the components of a framed tangle be pairwise disjoint.

As with framed links, we disallow "Möbius" tangles. Let a, b, c, d be the four corners of $I \times I$ such that $a = (0, 0), b = (1, 0), c = (1, 1)$, and $d = (0, 1)$. In W, these points inherit a cyclic ordering and we require that this ordering be (a, b, c, d). This prevents the components of T with boundary from having "half-twists." For example, we do not allow the framed tangle shown in Figure 17, where the gray circle represents $W^+ \cup W^-$.

We say that tangles T and T' are **isotopic** if there exists a smooth isotopy $H : B \times I \to B$ such that

1. $H|_{B\times 0} = \mathrm{id}_B$

2. $H|_{B\times 1}(T_1) = T_2$

3. $H|_{W\times t}$ maps $W \to W$, $W^+ \to W^+$, and $W^- \to W^-$ for each time $t \in I$.

This definition extends immediately to oriented and framed tangles. For oriented tangles, the orientations in **2.** must agree. We remark that, although a tangle T might have boundary, our definition does not require it. Thus, every link is a tangle and tangles serve as a natural generalization of links.

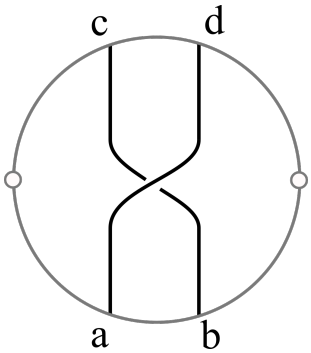

Figure 17.

We also consider tangle diagrams. Let D^2 be the unit disk in $\mathbb{R}^2$ with boundary circle S^1. A **tangle diagram** D_T is a 1-manifold with boundary, immersed in D^2 such that all points of self-intersection are transversal double points, $\partial D_T \subset S^1 \setminus \{(\pm 1, 0)\}$, and $D_T \pitchfork S^1$. If each component of D_T is given an orientation, D_T is called an **oriented tangle diagram**.

Framed tangle diagrams have a similar definition to framed link diagrams. A **framed tangle diagram** is a tangle diagram D_T that has been given the blackboard framing. In this case, the blackboard framing defines immersed annuli for the closed components of D_T and immersed rectangles for those components with boundary. As with framed link diagrams, when drawing framed tangle diagrams, we draw them as tangle diagrams and implicitly assume the blackboard framing.

The proof that every tangle diagram corresponds to a unique isotopy class of tangles and that every isotopy class of tangles can be presented by a tangle diagram is similar to that for links. The same is true in the oriented and framed cases. When drawing tangle diagrams, we include the image of S^1 for reference.

To illustrate the reason for some of our restrictions, consider Figure 18. If we did not require that an isotopy of tangles preserve inputs and outputs and their ordering, the two tangles shown would

be isotopic. To see why, note that we can produce the right tangle from the left by interchanging the

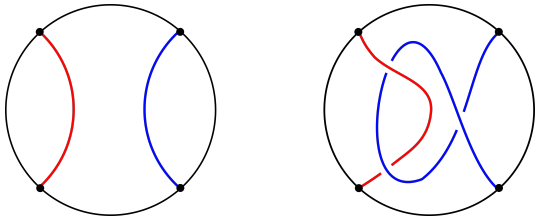

Figure 18.

northeast and northwest boundary points twice before interchanging the northeast and southeast boundaries once. Tangles constructed in this way, by permuting a fixed set of boundary points, form an important class of tangles called **rational tangles**. These can be classified according to the interchanges made. However, determining whether a given tangle is, in fact, a rational tangle is not straightforward. Classifying generic tangles is the focus of Chapter IX.

We now wish to study how two tangles might combine to form a link. Note that the closure of $S^3 \setminus B$ is another 3-ball, which we denote B_c. Moreover, $\partial B = \partial B_c$ and so we can define tangles in B_c just as in B. That is, a tangle $T' \in B_c$ is a smooth 1-manifold with boundary, embedded in B_c such that, $T' \pitchfork S^2$ and $\partial T' \subset W \setminus \{(\pm 1, 0, 0)\}$, where W is defined as above.

We say that a tangle T in B **embeds** in a link L if there exists a tangle T' in B_c such that $\partial T = \partial T'$ and $T \cup T' = L$ up to isotopy. In this case, we also say that T' **completes** T to form L. For example, considering the right–hand tangle in Figure 18 as a tangle in B_c, we would say the left–hand tangle embeds in a link known as the Hopf link, as shown in Figure 19. In fact, every rational tangle embeds in every link.

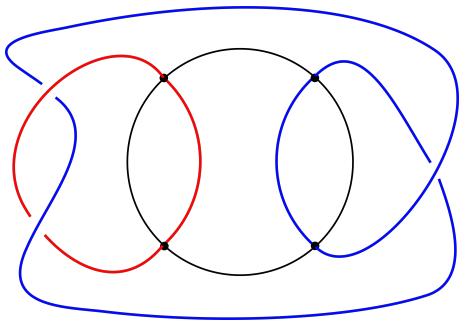

Figure 19.

We can also define tangles in the standard solid torus. Let $M \cong D^2 \times S^1$ denote the solid torus obtained by revolving the region $\{(x, 0, z) : (x-2)^2 + z^2 \leq 1\}$ about the z-axis in S^3. Let Γ be the outer

component of $M \cap xy$-plane. That is, Γ is the longitude of M of maximal diameter. A **genus-1 tangle** T_g is a compact, smooth 1-manifold with boundary, embedded in M such that $\partial T_g \subset \Gamma \setminus \{(-3,0,0)\}$. Starting at $(-3,0,0)$ and traveling around Γ in the positive x-direction through the upper half-plane in the xy-plane, the boundary points of T_g inherit an ordering. We say that two genus-1 tangles T_g and T_g' are **isotopic** if there exists an isotopy $H : M \times I \to M$ such that

1. $H|_{M\times 0} = \mathrm{id}_M$
2. $H|_{M\times 1}(T_g) = T_g'$
3. $H|_{\Gamma\times t}$ maps $\Gamma \to \Gamma$ bijectively and preserves the order the boundary points for each time $t \in I$.

Both **oriented** and **framed genus-1 tangles** have the expected definitions.

The closure of $S^3 \setminus M$ is again a copy of $D^2 \times S^1$, which we denote M_c. Genus-1 tangles in M_c are defined similarly and we again require that their boundaries be contained in $\Gamma \setminus \{(-3,0,0)\}$. We say that a genus-1 tangle $T_g \subset M$ **embeds** in a link L if there exists a genus-1 tangle $T_g' \subset M_c$ such that $\partial T_g = \partial T_g'$ and $T_g \cup T_g' = L$. In Chapter VII, we study a question, originally posed by Krebes, that asks whether a specific genus-1 tangle embeds in the unknot.

CHAPTER VI

QUANTUM TOPOLOGY

To study tangles, we now introduce some basic notions of quantum topology. The underlying technique used in quantum topology assigns, to a given tangle diagram, a sequence of vector spaces and linear maps. Depending on the linear maps chosen, their composition then gives various knot invariants. These are known as **operator invariants** of knots. For example, the Kauffman bracket, Jones polynomial, and Alexander polynomial can all be formulated as operator invariants. We will need a slightly modified, though equivalent, definitions of tangles and tangle diagrams. We draw upon the discussions in [10] and [15].

A **tangle** T is a compact 1-manifold with boundary, embedded in $\mathbb{R}^2 \times [0,1]$ such that the boundary of T is contained in $\{0\} \times \{1,2,\dots\} \times \{0,1\}$ and $T \pitchfork (\mathbb{R}^2 \times \{0,1\})$. Two tangles T_1 and T_2 are said to be **isotopic** if there is a smooth isotopy of $\mathbb{R} \times \mathbb{R} \times [0,1]$ taking T_1 to T_2 and fixing the boundary $\mathbb{R} \times \mathbb{R} \times \{0,1\}$. We require that both the inputs and outputs fall on consecutive, increasing integer points starting at $(0,1,1)$ and $(0,1,0)$ respectively. For example, every tangle with 3 inputs has inputs $\{(0,1,1),(0,2,1),(0,3,1)\}$ and no tangle has inputs $\{(0,3,1),(0,4,1),(0,5,1)\}$ or $\{(0,1,1),(0,3,1),(0,4,1)\}$. If each component of a tangle T has an orientation, then we say that T is an **oriented tangle**.

If each component of a tangle T is given a framing, we say that T is a **framed tangle**. For the closed components of T, this has the same definition as above. On the other hand, suppose that C is a component of T with boundary and let I be the unit interval $[0,1]$. A framing for C is a choice of embedding $I \times I \to \mathbb{R}^2 \times [0,1]$ such that $\{1/2\} \times I = C$, $(I \times I) \cap (\{0\} \times \mathbb{R} \times \{0,1\}) = I \times \{0,1\}$, and $I \times I \pitchfork \{0\} \times \mathbb{R} \times \{0,1\}$. More specifically, suppose that $\partial C = \{(0,j,\alpha),(0,k,\beta)\}$ where $\alpha, \beta \in \{0,1\}$. We require that the four corners of $I \times I$ map to $\{(0, j \pm 1/4, \alpha), (0, k \pm 1/4, \beta)\}$. The **$j$-framing** for C is an embedding of $I \times I$ that twists j times around its central axis. As in the previous section, we disallow "Möbius" tangles that incorporate a half-twist. Of course, we require that the components of a framed tangle be pairwise disjoint.

A **tangle diagram** D is a compact 1-manifold with boundary, immersed in $\mathbb{R} \times [0,1]$ such that the boundary of D is contained in $\{1,2,\dots\} \times \{0,1\}$ and $D \pitchfork (\mathbb{R} \times \{0,1\})$. As before, it can be shown that every tangle diagram corresponds to a unique tangle up to isotopy and that every isotopy class of tangles can be represented by a tangle diagram. An **oriented** tangle diagram is a tangle diagram in which each component is assigned an orientation.

A **framed tangle diagram** is a tangle diagram D that has been given the blackboard framing. A framed tangle diagram thus consists of immersed rectangles and annuli in $\mathbb{R} \times [0,1]$ together with the crossing information inherited from D. We add the additional constraint that, if C is a component of D such that $\partial C = \{(j,\alpha),(k,\beta)\}$ for $\alpha, \beta \in \{0,1\}$, then the corners of the immersed rectangle corresponding to C are exactly the four points $\{(j \pm 1/4, \alpha), (k \pm 1/4, \beta)\}$. Later, this will allow us to compose framed tangle diagrams without ambiguity. As before, when drawing framed tangle diagrams, we draw them as tangled diagrams and assume the blackboard framing.

If D is a tangle diagram, we call the boundary points of D contained in $\{1,2,\dots\} \times \{1\}$ **inputs** and boundary points of D in $\{1,2,\dots\} \times \{0\}$ **outputs**. As with tangles, we require that both the inputs and outputs fall on consecutive, increasing integer points starting at $(1,1)$ and $(1,0)$ respectively. Two tangle diagrams D and D' are **isotopic** if there is an isotopy of $\mathbb{R} \times [0,1]$ taking D to D' and fixing $\mathbb{R} \times \{0,1\}$. This definition applies equally well to oriented and framed tangle diagrams. In the oriented case, the orientations of D and D' must agree.

We will study framed tangles via framed tangle diagrams by considering framed tangle diagrams to be the morphisms in a category. Recall that a **category C** consist of the following data:

1. a class $\mathrm{Ob}(\mathbf{C})$, whose elements are called **objects** of $\mathbf{C}$
2. for any two objects $X, Y \in \mathrm{Ob}(\mathbf{C})$, there is a set $\mathrm{Hom}_{\mathbf{C}}(X,Y)$ whose elements are called **morphisms** and are represented by arrows $X \to Y$
3. for any three objects $X, Y, Z \in \mathrm{Ob}(\mathbf{C})$ there is a **composition** map

$$\mathrm{Hom}_{\mathbf{C}}(Y,Z) \times \mathrm{Hom}_{\mathbf{C}}(X,Y) \to \mathrm{Hom}_{\mathbf{C}}(X,Z)$$

   where the image of (g,f) is denoted $g \circ f$.
4. for every $X \in \mathrm{Ob}(\mathbf{C})$, there is a morphism $\mathrm{id}_X \in \mathrm{Hom}_{\mathbf{C}}(X,X)$ called the **identity** morphism

We require that $(h \circ g) \circ f) = h \circ (g \circ f)$ whenever the composition makes sense and that $f \circ \mathrm{id}_X = f = \mathrm{id}_Y \circ f$, whenever $f \in \mathrm{Hom}_{\mathbf{C}}(X,Y)$. We denote the set $\mathrm{Hom}_{\mathbf{C}}(X,X)$ by $\mathrm{End}_{\mathbf{C}}(X)$. When it is clear from the context, we simply write $\mathrm{Hom}(X,Y)$ and $\mathrm{End}(X)$. A map between categories is called a **functor**. Note that a functor is a map of both objects and morphisms. That is, if $\mathcal{F} : \mathbf{C} \to \mathbf{D}$ is a functor then for every pair of objects $X, Y \in \mathrm{Ob}(\mathbf{C})$ and every element $f \in \mathrm{Hom}_{\mathbf{C}}(X,Y)$ there exists a morphism $\mathcal{F}(f) \in \mathrm{Hom}_{\mathbf{D}}(\mathcal{F}(X), \mathcal{F}(Y))$.

We can also define the **product** of two categories $\mathbf{C}$ and $\mathbf{C}'$ to be the category $\mathbf{C} \times \mathbf{C}'$ given by

1. $\mathrm{Ob}\,(\mathbf{C} \times \mathbf{C}') = \mathrm{Ob}\,(\mathbf{C}) \times \mathrm{Ob}\,(\mathbf{C}')$.

2. $\mathrm{Hom}_{\mathbf{C}\times\mathbf{C}'}((X, X'), (Y, Y')) = \mathrm{Hom}_{\mathbf{C}}(X, Y) \times \mathrm{Hom}_{\mathbf{C}'}(X', Y')$ for all $X, Y \in \mathrm{Ob}\,(\mathbf{C})$ and $X', Y' \in \mathrm{Ob}\,(\mathbf{C}')$

3. composition defined by $(g, g') \circ (f, f') = (g \circ f, g' \circ f')$ and $\mathrm{id}_{(X,X')} = (\mathrm{id}_X, \mathrm{id}_{X'})$.

As an example of a category we might take **Top**, whose objects are topological spaces and whose morphisms are continuous maps. Another category is **Ab** whose objects are abelian groups and whose morphisms are group homomorphisms. An example of a functor would be the map that sends each topological space X to $H_1(X)$ and each continuous map $f : X \to Y$ to the induced homomorphism $f_* : H_1(X) \to H_1(Y)$.

We can now define the category **FD** of unoriented, framed tangle diagrams as follows. The elements of $\mathrm{Ob}\,(\mathbf{FD})$ are nonnegative integers, corresponding to the standard input and output points. For each pair of positive integers (j, k), the set $\mathrm{Hom}\,(j, k)$ consists of isotopy classes of framed tangle diagrams with m inputs and n outputs. The identity morphism $\mathrm{id}_j \in \mathrm{End}\,(j)$ is the isotopy class of j vertical line segments connecting the j inputs and j outputs. Note that $\mathrm{End}\,(0)$ consists of all isotopy classes of framed link diagrams.

If $f \in \mathrm{Hom}\,(j, k)$ and $g \in \mathrm{Hom}\,(k, l)$, the composition $g \circ f$ is defined to be the framed tangle diagram obtained by shifting f to be a diagram in $\mathbb{R} \times [1, 2]$, taking the union $g \cup f$ in $\mathbb{R} \times [0, 2]$, smoothing any corners if necessary, and shrinking the result by a vertical factor of 2 as depicted in Figure 20. Note that this composition is defined only if g has the same number of inputs as f has outputs. This

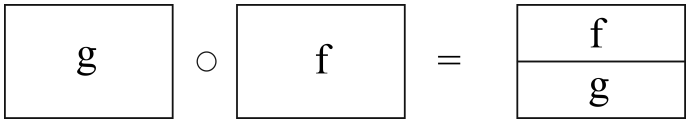

Figure 20.

composition is associative and thus **FD** is indeed a category.

However, we can go further and give **FD** the structure of a strict monoidal category. A **strict monoidal category** is a category $\mathbf{C}$ endowed with a functor $\otimes : \mathbf{C} \times \mathbf{C} \to \mathbf{C}$, called the **monoidal product** and an object $\mathbb{1} \in \mathrm{Ob}\,(\mathbf{C})$, called the **unit object** such that for any $X, Y, Z \in \mathrm{Ob}\,(\mathbf{C})$,

1. $(X \otimes Y) \otimes Z = X \otimes (Y \otimes Z)$

2. $\mathbb{1} \otimes X = X \otimes \mathbb{1} = X$

3. $(f \otimes g) \otimes h = f \otimes (g \otimes h)$ for any morphisms f, g and h

4. $(f' \circ f) \otimes (g' \circ g) = (f' \otimes g') \circ (f \otimes g)$ for any morphisms such that

$$X \xrightarrow{f} X' \xrightarrow{f'} X'' \quad \text{and} \quad Y \xrightarrow{g} Y' \xrightarrow{g'} Y''$$

5. $\mathbb{1}_X \otimes \mathbb{1}_Y = \mathbb{1}_{X \otimes Y}$.

In the case of **FD**, the monoidal product map, which we will refer to as the **tensor product**, is easily defined. For any integers $j, k \in \mathrm{Ob}(\mathbf{FD})$, $j \otimes k = j + k$ and if diagrams f and g are such that $f : j \to j'$ and $g : k \to k'$ then $f \otimes g : j + k \to j' + k'$ and is defined by juxtaposition as shown in Figure 21. Note that it is not necessarily the case that $f \otimes g = g \otimes f$. The unit object in **FD** is the empty diagram

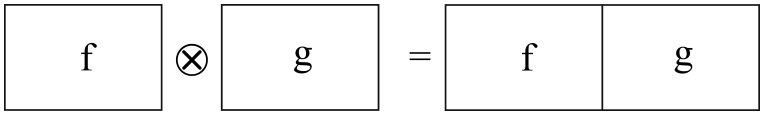

Figure 21.

with 0 inputs and 0 outputs. It is straightforward to check that this gives **FD** the structure of a monoidal category.

Now that we may combine framed tangle diagrams both via composition and via the $\otimes$ map, it is natural to ask what a generating set might be. The answer is remarkably simple.

Theorem 5. *The framed tangle diagrams shown in Figure 22, known as the* ***elementary tangle diagrams****, generate* **FD**.

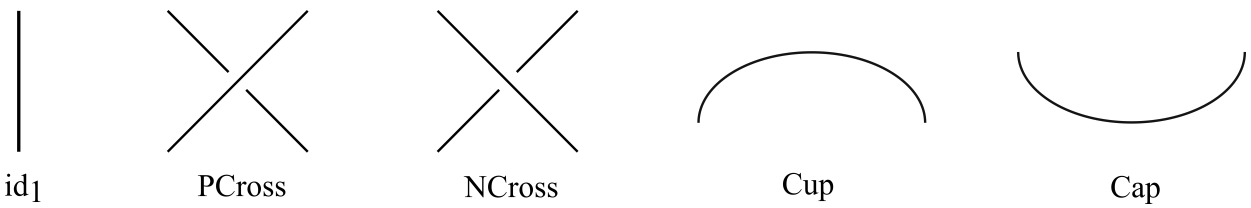

Figure 22.

Sketch of Proof: Let D be a framed tangle diagram of n crossings. Using Sard's Theorem, it can be shown that D is isotopic to a diagram D' with n crossings and a finite number k many quadratic critical points with respect to the height function $\mathbb{R} \times [0,1] \to [0,1]$. After an isotopy of the plane that preserves these critical points, we may find a partition $\{0 = t_0 < t_1 < t_2 < \cdots < t_{n+k} < t_{n+k+1} = 1\}$ of $[0,1]$, such that each sub-diagram $D_i = D \cap (\mathbb{R} \times [t_i, t_{i+1}])$ consists of the disjoint union of vertical segments and either one crossing or one critical point for each $i = 0, 1, 2, \ldots, n+k$. A framed tangle diagram in this form is called a **sliced diagram**. We see that each D_i is itself a framed tangle diagram, isotopic to either id_j for some integer j or the tensor product of some number of copies of id_1 and exactly one of the other four elementary diagram. We call diagrams of this form **basic diagrams**. Because $D = D_{n+k+1} \circ D_{n+k} \circ \cdots \circ D_1 \circ D_0$ and because D was arbitrary, we have shown that the elementary tangle diagrams generate **FD**. $\square$

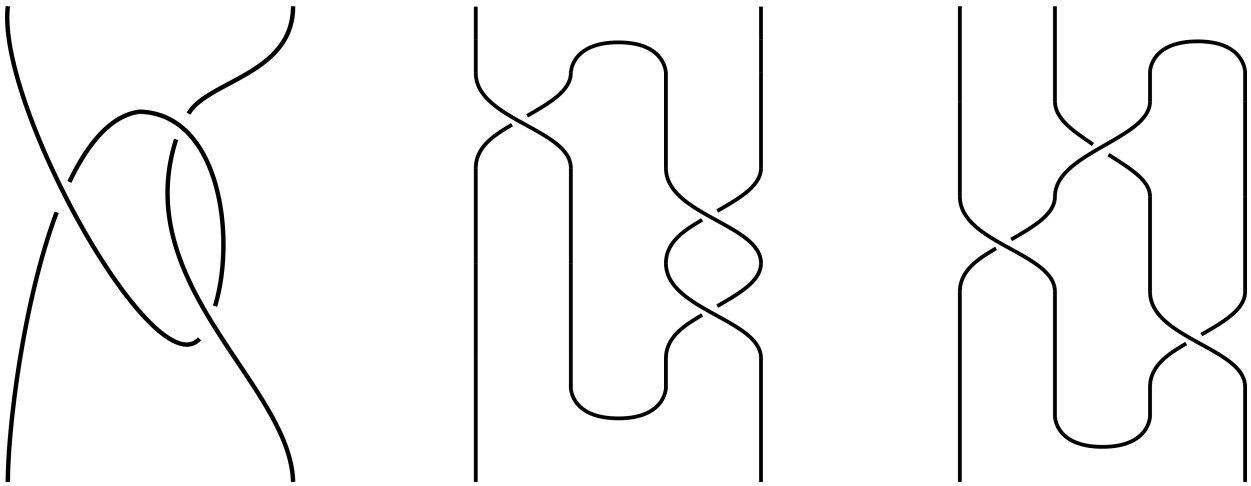

Figure 23.

In general, when given a framed tangle diagram D, we assume that it is a sliced diagram. However, distinct sliced diagrams may present isotopic framed tangles as seen in Figure 23. As we intend to study framed tangles through tangle diagrams, we need a method to determine when two sliced diagrams present the same isotopy class of framed tangles.

The following theorem might be thought of as the analogue to Reidemeister's theorem in the context of sliced, framed tangle diagrams. The set of diagrammatic moves used incorporate the Reidemeister moves and are known as the **Turaev moves**. Turaev's original proof of the following theorem can be found in [14] and an accessible outline can be found in [10].

Theorem 6. *Two framed, sliced diagrams D and D' present the same isotopy class of framed tangles if and only if they are related by a finite sequence of the moves shown in Figure 24 together with the framed Reidemeister moves.*

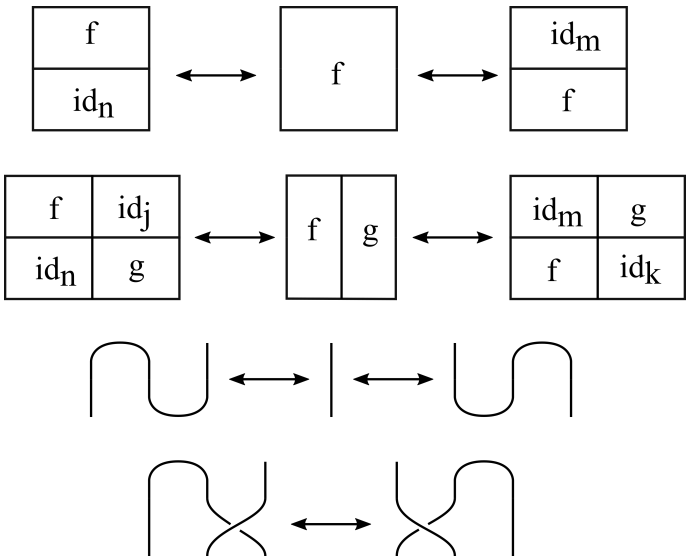

Figure 24. $f \in \mathrm{Hom}\,(m,n)$ and $g \in \mathrm{Hom}\,(j,k)$

This result allows us to apply linear algebra. More explicitly, we generalize the Kauffman bracket to framed tangle diagrams via a functor with domain **FD**. Let $\mathbb{F}$ be a field and let $\mathbf{Vect}_{\mathbb{F}}$ be the category of finite dimensional vector spaces over $\mathbb{F}$. Morphisms in this category are linear maps. Let V be a 2-dimensional vector space over $\mathbb{F}$ with basis $\{e_0, e_1\}$. Note that $V \otimes V$ then has basis $\mathcal{B} = \{e_0 \otimes e_0, e_0 \otimes e_1, e_1 \otimes e_0, e_1 \otimes e_1\}$.

Let A be any nonzero element of $\mathbb{F}$. We define a functor $\mathcal{K}_A : \mathbf{FD} \to \mathbf{Vect}_{\mathbb{F}}$ known as the **bracket functor**. Because they generate **FD**, it suffices to define $\mathcal{K}_A$ on the elementary tangle diagrams and require that $\mathcal{K}_A$ respects the tensor product structure of $\mathcal{K}_A$. That is, for any two objects we require $\mathcal{K}_A(m \otimes n) = \mathcal{K}_A(m) \otimes \mathcal{K}_A(n)$ and for any two morphisms f and g in **FD**, we should have $\mathcal{K}_A(f \otimes g) = \mathcal{K}_A(f) \otimes \mathcal{K}_A(g)$. Note that the tensor on the left–hand side of each equation refers to the monoidal product in **FD** while the right–hand tensor signifies the monoidal product in $\mathbf{Vect}_{\mathbb{F}}$, which is just the usual tensor product of either two linear spaces or linear maps.

Define $\mathcal{K}_A$ by the following:

i. $\mathcal{K}_A(0) = \mathbb{F}$

ii. $\mathcal{K}_A(1) = V$

iii. $\mathcal{K}_A(\mathrm{id}_1) = \mathrm{id}_V$

iii. $\mathcal{K}_A(Cup) = n$ where $n \in \mathrm{Hom}_{\mathbf{Vect}_\mathbb{F}}(\mathbb{F}, V \otimes V)$ and is given by the matrix

$$n = \begin{pmatrix} 0 \\ -A \\ A^{-1} \\ 0 \end{pmatrix} \tag{6.1}$$

iv. $\mathcal{K}_A(Cap) = u$ where $u \in \mathrm{Hom}_{\mathbf{Vect}_\mathbb{F}}(V \otimes V, \mathbb{F})$ and is given by the matrix

$$u = \begin{pmatrix} 0 & A & -A^{-1} & 0 \end{pmatrix} \tag{6.2}$$

v. $\mathcal{K}_A(PCross) = R$ where $R \in \mathrm{Hom}_{\mathbf{Vect}_\mathbb{F}}(V \otimes V, V \otimes V)$ and is given by the matrix

$$R = \begin{pmatrix} A & 0 & 0 & 0 \\ 0 & 0 & A^{-1} & 0 \\ 0 & A^{-1} & A - A^{-3} & 0 \\ 0 & 0 & 0 & A. \end{pmatrix} \tag{6.3}$$

vi. $\mathcal{K}_A(NCross) = R^{-1}$.

When the maps n, u, R, and R^{-1} are written as matrices, it is understood to be with respect to the basis $\mathcal{B}$. Each elementary diagram, together with its image under $\mathcal{K}_A$ is shown in Figure 25. Note that relation **ii.**, together with our requirement that $\mathcal{K}_A$ respect the monoidal product structure of **FD**, implies that $\mathcal{K}_A(m)$ is the m-fold tensor product of V with itself, which we denote $V^{\otimes m}$.

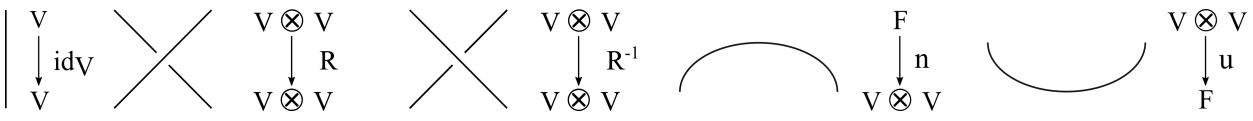

Figure 25.

This raises a minor technical problem which we mention briefly. Whereas **FD** is a *strict* monoidal category, $\mathbf{Vect}_{\mathbb{F}}$ is not. This causes the following ambiguity,

$$\mathcal{K}_A(m \otimes n) = \mathcal{K}_A(m+n) = V^{\otimes(m+n)} \neq V^{\otimes m} \otimes V^{\otimes n} = \mathcal{K}_A(m) \otimes \mathcal{K}_A(n) = \mathcal{K}_A(m \otimes n). \tag{6.4}$$

However, the vector spaces $V^{\otimes(m+n)}$ and $V^{\otimes m} \otimes V^{\otimes n}$ are canonically isomorphic. Hence, whenever a situation of this type arises, we implicitly compose our maps with the appropriate canonical isomorphism.

We have now defined $\mathcal{K}_A$ on elementary diagrams. However, as we hope to study framed tangles and not just their diagrams, we need the following result.

Theorem 7. *If D and D' present isotopic framed tangles, then $\mathcal{K}_A(D) = \mathcal{K}_A(D')$.*

Proof: This proof is a straightforward computation. One shows that if D is a sliced diagram, and D' is any diagram obtained from D via one of the Turaev moves, then $\mathcal{K}_A(D) = \mathcal{K}_A(D')$. As it will be useful in what follows, we show that $\mathcal{K}_A$ is invariant under the framed RI move.

As a sliced diagram, the unframed RI move has either of the following descriptions:

$$\mathrm{id}_1 \leftrightarrow (\mathrm{id}_1 \otimes Cap) \circ (PCross \otimes \mathrm{id}_1) \circ (\mathrm{id}_1 \otimes Cup) \quad \text{or} \tag{6.5}$$

$$\mathrm{id}_1 \leftrightarrow (\mathrm{id}_1 \otimes Cap) \circ (NCross \otimes \mathrm{id}_1) \circ (\mathrm{id}_1 \otimes Cup). \tag{6.6}$$

The relations in lines (6.5) and (6.6) correspond to the left–hand and right–hand tangles shown in Figure 26. Applying $\mathcal{K}_A$, we find

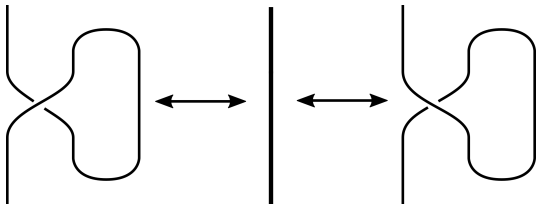

Figure 26.

$$(\mathrm{id}_V \otimes n) \circ (R \otimes \mathrm{id}_V) \circ (\mathrm{id}_V \otimes u) = \begin{pmatrix} -A^3 & 0 \\ 0 & -A^3 \end{pmatrix} = (-A^3)\mathrm{id}_V \tag{6.7}$$

$$(\mathrm{id}_V \otimes n) \circ (R^{-1} \otimes \mathrm{id}_V) \circ (\mathrm{id}_V \otimes u) = \begin{pmatrix} -A^{-3} & 0 \\ 0 & -A^{-3} \end{pmatrix} = (-A^{-3})\mathrm{id}_V. \tag{6.8}$$

Compare this to Lemma 4. It now follows that if a tangle diagram D' is obtained from a diagram D via a framed RI move, then

$$\mathcal{K}_A(D') = (-A^3)(-A^{-3})\mathcal{K}_A(D) = \mathcal{K}_A(D). \tag{6.9}$$

Hence, the bracket functor is an invariant of framed tangles. □

The following theorem relates the $\mathcal{K}_A$ to the Kauffman bracket as defined in Chapter III.

Theorem 8. *If D is a sliced diagram presenting a link L, then $\mathcal{K}_A(D)$ represents the unreduced Kauffman bracket of L.*

Proof: As in Chapter III, let D_0 be a diagram of the unknot with no crossings. To define the unreduced Kauffman bracket, we set $\langle D_0 \rangle = -A^2 - A^{-2}$ yet still use the defining relations **ii.** and **iii.** shown in Figure 13.

Note that $D_0 = Cap \circ Cup$. Hence,

$$\mathcal{K}_A(Cap \circ Cup) = u \circ n = -A^2 - A^{-2}. \tag{6.10}$$

The skein relation also holds as

$$A(\mathcal{K}_A(\mathrm{id}_2)) + A^{-1}(\mathcal{K}_A(Cup \circ Cap)) = A\mathrm{id}_{V\otimes V} + A^{-1}(u \circ n) \tag{6.11}$$

$$= A \begin{pmatrix} 1 & 0 & 0 & 0 \\ 0 & 1 & 0 & 0 \\ 0 & 0 & 1 & 0 \\ 0 & 0 & 0 & 1 \end{pmatrix} + A^{-1} \begin{pmatrix} 0 & 0 & 0 & 0 \\ 0 & -A^2 & 1 & 0 \\ 0 & 1 & -A^2 & 0 \\ 0 & 0 & 0 & 0 \end{pmatrix} \tag{6.12}$$

$$= R = \mathcal{K}_A(PCross). \qquad \square \tag{6.13}$$

CHAPTER VII

PD CODES

We being our computational work with tangles. To do this, we use the Knot Theory package for Mathematica which can be found at [9].

Central to our ability to analyze knots within Mathematica are PD codes, which can be thought of as an $n \times 4$ integer matrices that correspond to oriented link diagrams. The method for generating a PD code for a given oriented link diagram D is as follows.

Suppose that D is an oriented link diagram of n crossings. Ignoring the over/under crossing information, D is a directed, 4-valent graph of n vertices such that at each vertex v, two edges arrive and two edges depart. Label each edge of D with a unique integer chosen from $1, 2, \ldots, 2n$. The choice of labelling is immaterial. Label each vertex v with the symbol $X[a, b, c, d]$ such that

1. a corresponds to the arriving under branch in the original link diagram D

2. starting at a and traveling counter clockwise around v, the edges b, c, and d appear in that order.

An example of how the crossings are labelled is shown in Figure 27. A **PD code** for an oriented link

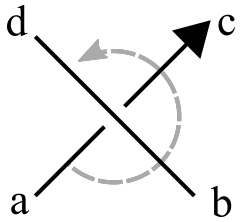

Figure 27.

diagram D of n crossing is then the collection of the n symbols $\{X[a_i, b_i, c_i, d_i]\}_{i=1}^{n}$.

Suppose that $PD = \{X[a_i, b_i, c_i, d_i]\}_{i=1}^{n}$ is a PD code corresponding to an oriented link diagram D of n crossings. Each label $X[a_i, b_i, c_i, d_i]$ encodes the orientation of the under crossing. However, the over crossing might have either of the two possible orientations. Thus, as long as a component of D occurs as the under crossing at least once, PD encodes its orientation. If there is a component of D that does not occur as an under crossing, we can alter D by an $\overrightarrow{RII}$ move so that this component is the under crossings in two crossings. The corresponding PD code, PD' will then contain the information of its orientation. We can take the same approach if D contains a component that is not involved with any crossing.

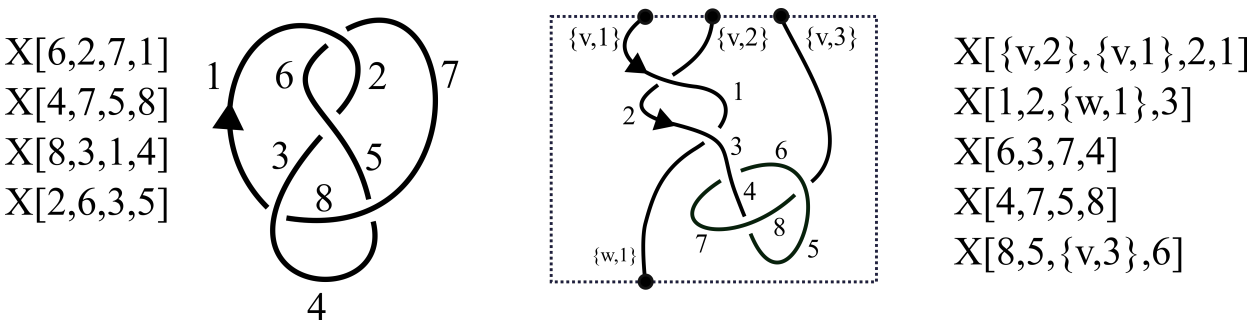

Figure 28.

We define PD codes for tangles similarly. Suppose that D is an oriented tangle diagram of k crossings, m inputs and n outputs. Ignoring the crossing information, D is an oriented graph with k 4-valent vertices and $m + n$ 1-valent vertices. We label the edge adjacent to the ith input $\{v, i\}$ and the edge adjacent to the jth output $\{w, j\}$, the labels v and w being formal labels corresponding to those in Chapter VI. The interior edges, ie. those edges not adjacent to an input or an output, are labelled with unique integers just as in the case for PD codes for links. The crossings are now labelled via the same rule as before. An example of a knot diagram and a tangle diagram and their corresponding PD codes is shown in Figure 28.

CHAPTER VIII

KREBES'S TANGLE

We now study a particular genus-1 tangle. Let $M = D^2 \times S^1$ be the standard solid torus in S^3, as defined in Chapter V. Consider the genus-1 tangle $\mathcal{A}$, known as Krebes's Tangle, which is shown in Figure 29 together with a longitude l of ∂M. It is often easier to depict $\mathcal{A}$, and genus-1 tangles in general, using tangle diagrams of the form shown in Figure 30. The boundary of M is shown in grey and the dot at the center of the figure represents the genus. That this diagram has corners is an aesthetic artifact.

Krebes first posed the following question in [7].

Question 1. *Does $\mathcal{A}$ embed in the unknot?*

Abernathy achieved a partial result in [1]. Let Σ be the disk in $S^3 \setminus M$ bounded by l. Using the Kauffman bracket skein module, Abernathy showed that if a genus-1 tangle T completes $\mathcal{A}$ to form the unknot, then it passes through Σ an even number of times. In other words, it passes through the hole of the donut an even number of times.

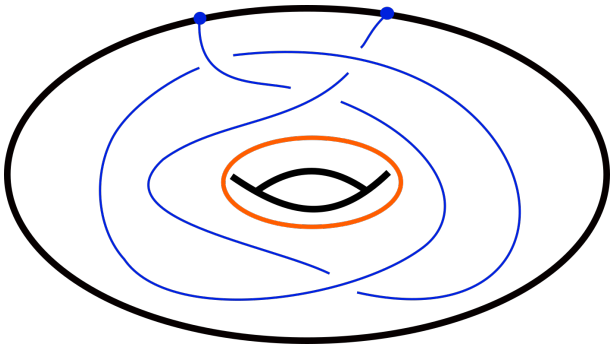

Figure 29. Krebes's Tangle

Our approach has been more computational. We have written code that generates random tangles and performs the gluing process using PD–codes. From there, we can calculate the Alexander and Jones polynomials of the resulting knots. Knots for with Alexander polynomial 1 have then been saved for further study.

As we are interested in completing Krebes's tangle, which has two boundary points and one component, to form the unknot, we restrict our attention to one component genus-1 tangles with nonempty boundary. Let M^c be the complimentary solid torus to M in S^3 and let T_g be a genus-1 tangle of one component in M^c such that $\partial\mathcal{A} = \partial T_g$. Let U be an open neighborhood of ∂T_g diffeomorphic to $(-1, 1) \times D^2$.

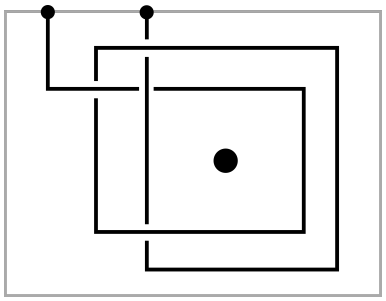

Figure 30.

Note that l is a meridian of M^c bounding the disk Σ in M^c. Performing an isotopy of T_g if necessary, we may assume that $T_g \pitchfork \Sigma$. As T_g is compact $T_g \cap \Sigma$ is a finite collection of points. Moreover, there exists an open neighborhood $W \subset M^c$ of $T_g \cap \Sigma$ homeomorphic to $(-1,1) \times D^2$ such that, after a local isotopy of T_g in a neighborhood of W, $T_g \cap \overline{W}$ consists of a disjoint union of line segments in the xy-plane. Hence, after smoothing the corners of $\overline{W}$ and $\overline{M^c \setminus W}$, we will have decomposed T_g as the union of a tangle T with $2m+2$ boundary points and an m-component untangle S. The result is a presentation of T_g as shown in Figure 31.

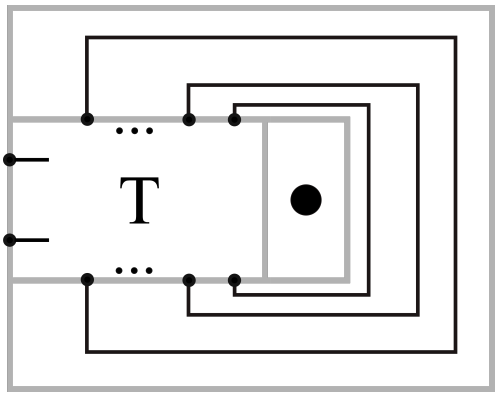

Figure 31.

We have now translated our study of genus-1 tangles to one of studying tangles in the standard 3-ball. Suppose that T_g is a genus-1 tangle such that $T_g = T \cup S$ where T and S are as before and T has $2m+2$ boundary points. When completing $\mathcal{A}$ with T_g, m corresponds to the number of times T_g passes through Σ. Abernathy's result now tells us that if T_g completes $\mathcal{A}$ to form the unknot then m must be even. We can therefore restrict our attention to tangles T with $2m+2$ boundary components for even m.

We now describe how we generate random tangles using PD codes. Suppose that T and T' are tangles with PD codes PT and PT' respectively. Suppose that T has j outputs $\{\{w,i\}_{i=1}^{j}\}$ and

T' has k inputs $\{\{v,i\}_{i=1}^{k}\}$. After specifying to which output $\{v,1\}$ should be identified, our program $GlueTangleAt$ glues consecutive outputs to consecutive inputs. For example, $GlueTangleAT[PT, PT', 2]$ would glue $\{v,1\}$ to $\{w,2\}$, and $\{v,2\}$ to $\{w,3\}$, and so on. If any inputs or outputs are not glued, they become inputs or outputs respectively in the composite tangle. All interior edges in the composite tangle are completely relabeled at random. Figure 32 shows the example of $GlueTangleAt[PT, PT', 2]$ where $k = j = 3$.

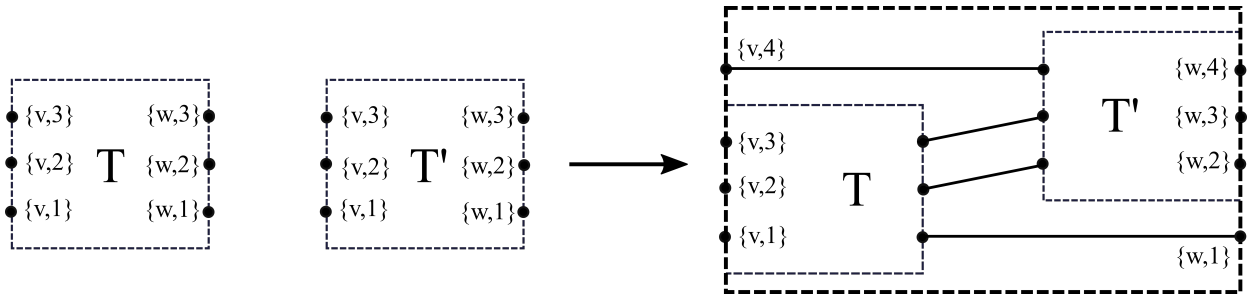

Figure 32.

We can now generate random tangles by glueing together random strings of basic tangles. Our program $RandomTangle[n, y]$ starts with an n-component untangle and glues on y-many elementary tangles by nesting the $GlueTangleAt$ function y-many times, each time selecting a random elementary tangle from $\{PCross, NCross, Cap, Cup\}$. When "glueing on" a Cup to a tangle T, we simply add a Cup in the appropriate location and shift the outputs of T accordingly. If at any point there are no more outputs, the process stops. We have also found it useful not only to incorporate but to favor the tangles $PTwist = PCross \circ PCross$ and $NTwist = NCross \circ NCross$ in the list of elementary tangles to be added. Without these, the tangles generated tend to be rather "un–tangled."

There is a technical point here. Recall that PD codes only encode information about those components involved in crossings. Hence, to have PD codes for an untangle or for a Cap or Cup we must introduce crossings. For an untangle, we introduce a sequence of RII moves and for Cup and Cap we introduce an RI move. The PD codes for each of the elementary tangles is shown below Figure 33.

Suppose that T is a random tangle generated this way with j inputs and k outputs. In order to embed T into a genus-1 tangle as in Figure 31, we need that $j = k$. Suppose that $j < k$. Our program $EvenOutTangle$ accomplishes this by sending $\{w, k-i\} \to \{v, j+i+1\}$ for $i = 0, 1, \ldots, (k-j)/2$. Considering T as a tangle in B^3, this shifts outputs to inputs but maintains the total ordering of the boundary points of T. If $k < j$, the reverse operation occurs, sending inputs to outputs.

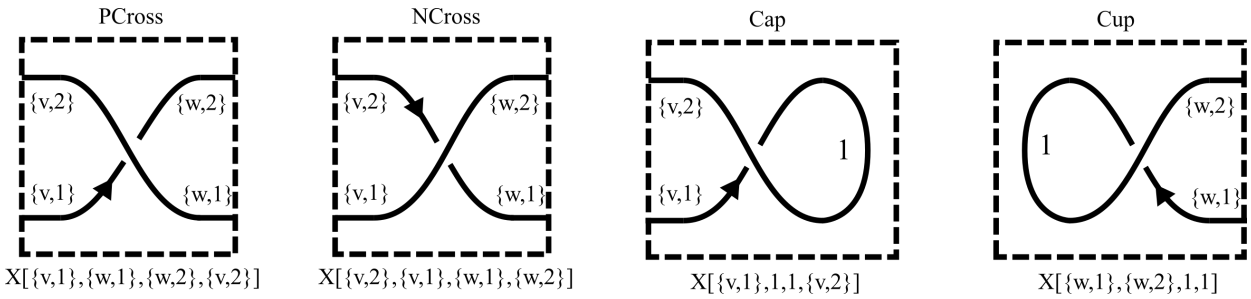

Figure 33.

We are now ready to convert our randomly generated tangles into genus-1 tangles and to use them to complete $\mathcal{A}$. These tasks are accomplished simultaneously. Let T be a random tangle with $m+1$ inputs and $m+1$ outputs. The boundary points $\{v,1\}$ and $\{w,1\}$ will be those that are glued to the boundary of $\mathcal{A}$. Hence, when we embed T in a genus-1 tangle T_g, we will do so by taking the union of T with an m-component untangle.

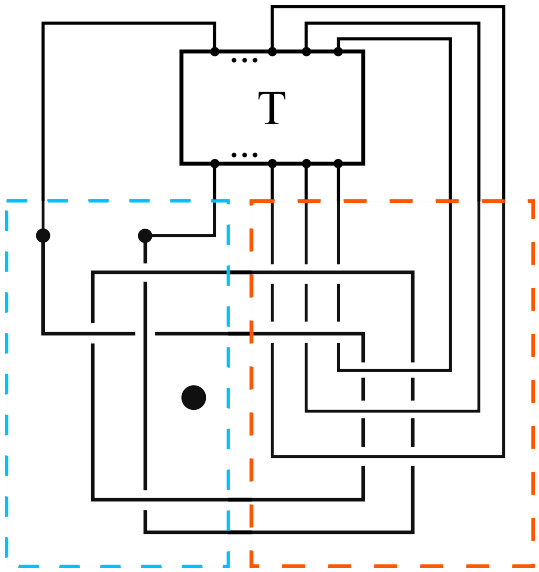

Figure 34.

However, the gluing process is not as simple as the process of gluing two tangles together. Let T be a random tangle and let $T_g \subset M^c$ be the tangle formed by completing T with an untangle. Figure 34 shows how the diagram of $\mathcal{A} \cup T_g$ contains additional crossings for each time T_g pass through Σ. To account for these additional crossings, we decompose the gluing into a process that involves gluing three tangles together.

Ignoring the genus, Figure 34 shows the component tangles to be glued. Denote the lower–left and lower–right tangles $K1$ and $K2$ respectively. Note that $K1$ does not depend on the random tangle T. On the other hand, $K2$ depends on the number of inputs and outputs of T. Thus, to perform the gluing, we generate a random tangle T, make equal its numbers of inputs and outputs, generate $K2$ according to this count, and glue all three tangles together. Our program *RandomKrebGlue* accomplishes each of these three steps.

We now have a means to randomly generate genus-1 tangles and use them to complete $\mathcal{A}$. However, before we can compute our polynomial invariants we must orient the resulting knots. For although we have glued our tangles together, we may have given our knot an inconsistent orientation. Our program *Orient*, gives the knot the orientation defined by the understrand of the first crossing listed in the PD code.

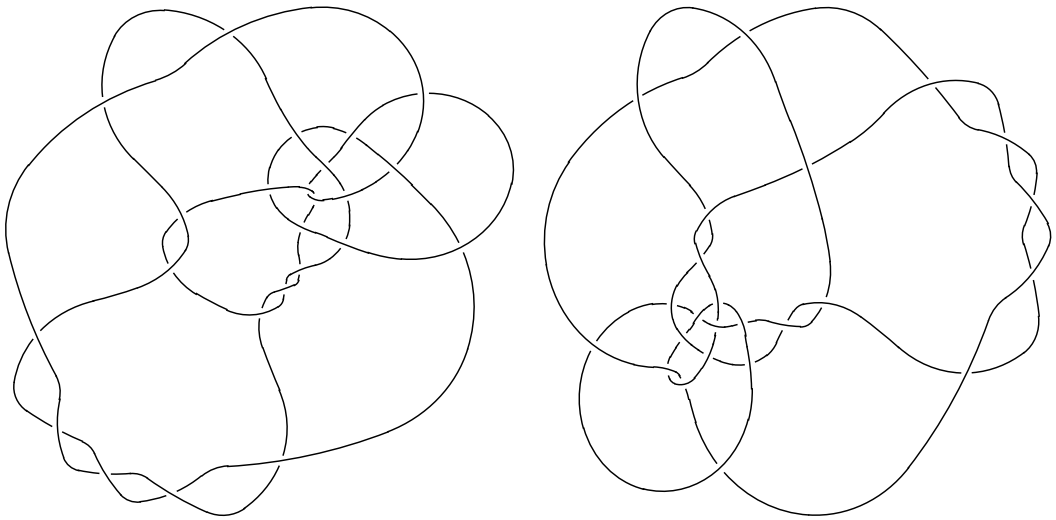

Figure 35.

Two examples of the result of the gluing are shown in 35. Note that in both cases, the planar diagrams are not minimal. That is, the number of crossings can be reduced via the $\overrightarrow{RI}$ and $\overrightarrow{RII}$ moves. This is often the case, partly due to chance and partly due to how our random tangles are generated. Recall that to express an n-component untangle as a PD code, we had to introduce a sequence of crossings that could all be undone with the $\overrightarrow{RII}$ move. This has the negative consequence of making the calculation of the Alexander and Jones Polynomials computationally expensive and thus limiting the number of trials we were able to run.

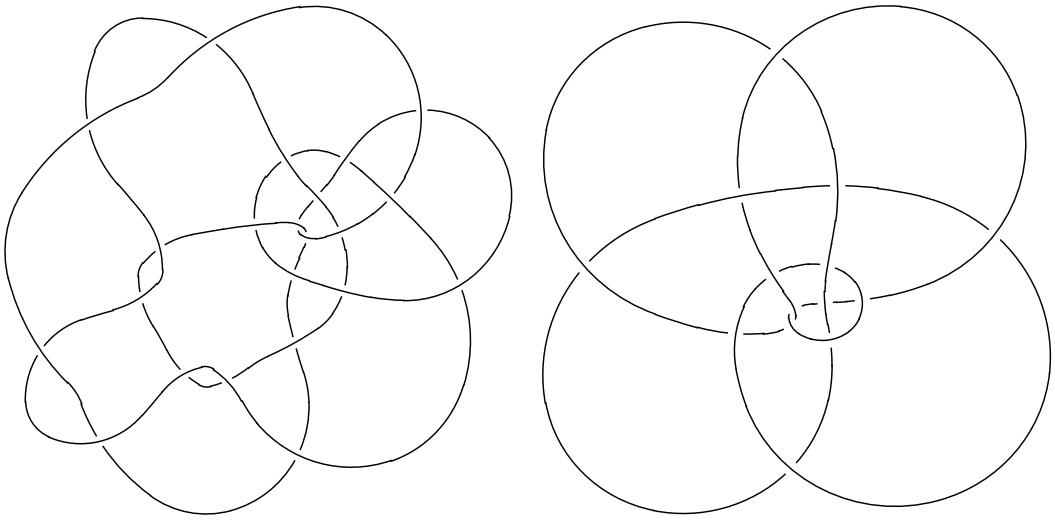

Figure 36.

In an attempt to counter act this, we have a code *RemoveAllReiderOnesAndTwos* that removes all the crossings that can be removed using the $\overrightarrow{RI}$ and $\overrightarrow{RII}$ moves. Unfortunately, this is computationally even worse, as at each time the program must test each crossing to see if it corresponds to an $\overrightarrow{RI}$ move and each pair of crossings to see if they correspond to an $\overrightarrow{RII}$ move. After removing one, the whole process must be repeated as potentially removing one unnecessary crossing exposed another. This happens, for example, when untwisting a sequence of twists followed by a *Cap*.

Nevertheless, *RemoveAllReiderOnesAndTwos* has proved useful. Once a knot K has been generated, we can run *RemoveAllReiderOnesAndTwos* to see a reduced presentation of the knot, from which it is simpler to see whether or knot K is the unknot. Figure 36 shows the result of one gluing before and after being reduced.

Thus far, we have tested approximately 2 million random tangles. Although we have found many with Alexander Polynomial 1, none have had Jones Polynomial 1. In the future, we hope to improve our efficiency both by editing our code and running it on a more powerful processor. Although this technique may not be able to give a definitive answer to Krebes's initial question, it has offered evidence toward the negative. More broadly, it has precipitated the development of software which can generate large random knots and tangles. We hope this to be useful to those studying knots and tangles in the future.

Finally, as an interesting aside, our program also provides an easy method to generate periodic links. An **n-periodic link** is a link L that is invariant under a rotation of $2\pi/n$ about an axis disjoint from L. Periodic links can be obtained by gluing a tangle, with j inputs and j outputs, to itself n-times before

identifying the resulting inputs and outputs in pairs. Given any tangle T and any positive integer n, our program *PeriodicLink* generates the n-periodic link obtained from T in this way. The link in Figure 1 is an example, as are those in Figure 37.

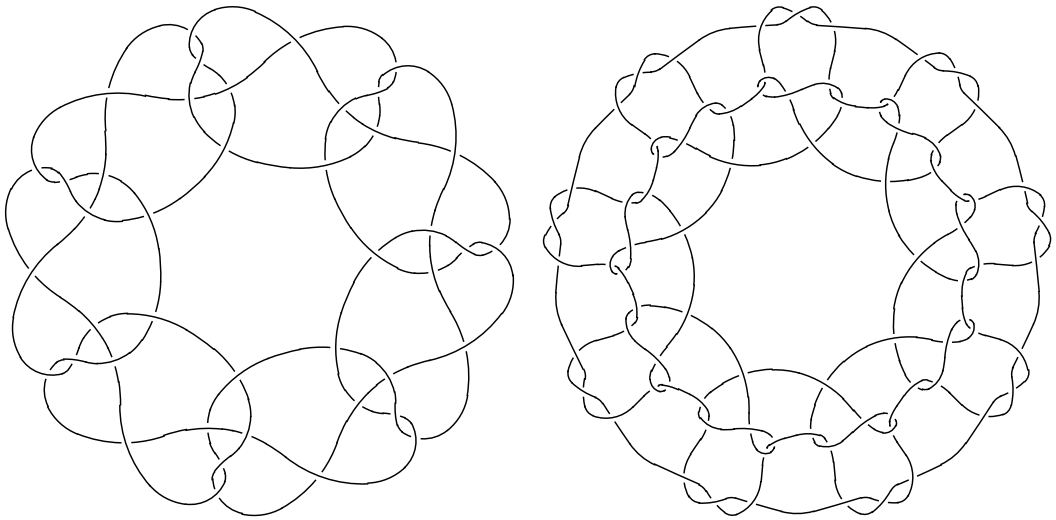

Figure 37.

CHAPTER IX

THE UNFRAMED KAUFFMAN BRACKET

In an on-going project, we have used the techniques of quantum topology, as well as the code described in the previous section to work toward producing a small census of unframed, unoriented, tangles in the three ball. To start, we construct an invariant coming from the Kauffman bracket functor.

Let $D \in \mathrm{Hom}_{\mathbf{FD}}(m,n)$. Then D is a framed, unoriented tangle diagram of m inputs and n outputs. Let $C_1,\dots,C_k$ be the components of D and let L be the framed tangle presented by D. For those components of D with no self–crossing, the blackboardboard framing presents the 0-framing of the corresponding component in L. We work to give those components with self–crossings the 0-framing.

There are 2^k possible ways to give D an orientation. Let the diagrams $\{D_j\}_{j=1}^{2^k}$ correspond to these oriented diagrams and let $\{C_i^j\}_{i=1}^{k}$ be the oriented components of D_j for $j = 1,\dots,2^k$. Suppose that C_i^j contains self–intersections and that $\omega(C_i^j) = k$, where ω represents the writhe as before. We now modify our tangle so that the writhe of each component is 0.

Write D as the composition of basic diagrams $f_l \circ \cdots \circ f_1$. Let $h_\alpha^+(n), h_\alpha^-(n) \in \mathrm{Hom}\,(n,n)$ be the diagrams shown in Figure 38, with a positive and negative crossing respectively, where the RI move occurs between $(\alpha,1)$ and $(\alpha,0)$. By giving $h_\alpha^\pm(n)$ the appropriate orientation, choosing the appropriate α, and inserting $h_\alpha^\pm(n)$ at an appropriate stage in the composition of the basic tangles f_i, we may alter the writhe of C_i^j by either ± 1. The result is a new diagram $D' = f_l \circ \cdots \circ h_\alpha^\pm(n) \circ \cdots f_1$. Note that both n and α depend on where in the composition $h_\alpha^\pm(n)$ is inserted.

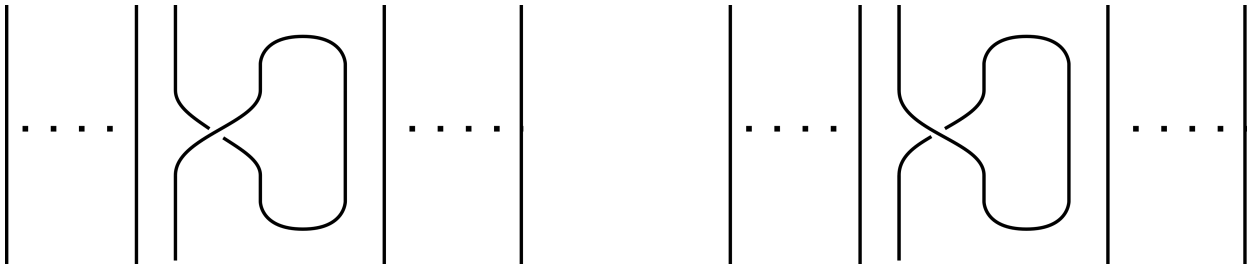

Figure 38.

Let us examine the effect this has on $\mathcal{K}_A(D)$. Following the proof of Theorem 7, for the $h_\alpha^\pm(n)$ tangles we find

$$\mathcal{K}_A(h_\alpha^+(n)) = (\mathrm{id}_V)^{\otimes\alpha-1} \otimes (-A^3)\mathrm{id}_V \otimes (\mathrm{id}_V)^{\otimes n-\alpha} \tag{9.1}$$

$$= (-A^3)(\mathrm{id}_V)^{\otimes n} \tag{9.2}$$

$$\mathcal{K}_A(h_\alpha^-(n)) = (\mathrm{id}_V)^{\otimes\alpha-1} \otimes (-A^{-3})\mathrm{id}_V \otimes (\mathrm{id}_V)^{\otimes n-\alpha} \tag{9.3}$$

$$= (-A^{-3})(\mathrm{id}_V)^{\otimes n}. \tag{9.4}$$

It follows that

$$\mathcal{K}_A(D') = \mathcal{K}_A(f_l) \circ \cdots \circ (-A^{\pm 3})\mathrm{id}_V \circ \cdots \mathcal{K}_A(f_1) = (-A^{\pm 3})\mathcal{K}_A(D). \tag{9.5}$$

Compare this to our construction of the Jones polynomial. Ignoring the framing, D' and D present isotopic unframed tangles. To unframe C_i^j, we can repeat this process according to $\omega(C_i^j)$ to find a new diagram D'' such that the component corresponding to C_i^j has the 0-framing and

$$\mathcal{K}_A(D'') = \left(-A^{-3\omega(C_i^j)}\right)\mathcal{K}_A(T). \tag{9.6}$$

We repeat this process on each component $\{C_i^j\}$ of D_j. Let $\omega(D_j) = \sum_i \omega(C_i^j)$ and define

$$K_j(D) = -A^{-3(\omega(D_j))}\mathcal{K}_A(D_j). \tag{9.7}$$

This is a linear transformation $V^{\otimes m} \to V^{\otimes n}$. Let T be an unoriented, unframed tangle and D a framed tangle diagram that, when the framing is ignored, presents T. The **unframed Kauffman bracket** of T is defined to be the collection of 2^k matrices,

$$\langle T \rangle_u = \{K_j(D)\}_{j=1}^{2^k}. \tag{9.8}$$

We have the following theorem.

Theorem 9. *The unframed Kauffman bracket is an isotopy invariant of unoriented, unframed tangles.*

Proof: We have seen that $\mathcal{K}_A$ is invariant under each of the Turaev moves, making it an isotopy invariant of framed tangles. To see that the oriented Kauffman bracket is an isotopy invariant for unframed tangles, it is only left to check that it is invariant under the unframed RI move. This is immediate from our construction. □

We can now use the oriented Kauffman bracket and our computational infrastructure to generate a small census of unframed, unoriented tangles. The first step is our program $RandomListTangle$ which generates a tangle diagram as a list of basic tangles in the form $\{\{m, \{\text{“}x\text{”}, i\}, n\}$. This is the basic tangle of m inputs, n outputs, and where the elementary tangle x occurs in the ith position. For example, one list tangle is,

{{3, {“Start”, 0}, 3}, {3, {“PCross”, 2}, 3}, {3, {“Cap”, 1}, 1}, {1, {“Cup”, 1}, 3}}.

A tangle in this list format corresponds to a sliced diagram D and from here it is easy to compute $\mathcal{K}_A(D)$. We simply translate each basic diagram to its image under $\mathcal{K}_A$ and multiply the resulting matrices. For example, $\{3, \{\text{“}PCross\text{”}, 2\}, 3\}$ becomes $\mathrm{id}_V \otimes R$.

Let T be the tangle presented by D. In order to compute $\langle T \rangle_u$ we must still orient D and compute the writhe of its components. To this end, our program $PDFromList$ uses the $GlueTangleAt$ program to generate a PD code from the list form of D. From this PD code, we can compute the number of components of D, find those components that contain self-crossings, and give D all of its possible orientations $\{D_j\}$. For each j, we then compute the writhe of the components of D_j and record the matrix $K_j(D)$. Doing this over all possible orientations, we find $\langle T \rangle_u$.

Finally, the “list tangle” format gives a combinatorial method for generating all possible tangle diagrams. We may now generate random tangle diagrams, compute the unframed quantum Kauffman bracket of the associated tangles, and sort them into equivalence classes based on the result. We hope this will produce a small census of tangles of small complexity. This work is ongoing.

APPENDIX

KNOTS OF ALEXANDER POLYNOMIAL 1

Here we show several knots in which Krebes's tangle embeds and which have Alexander Polynomial equal to 1. We show two planar diagrams for each knot, one "unreduced" and one "reduced" via our program *RemoveAllReiderOnesAndTwos*. Each is shown with its PD code.

—**A**—

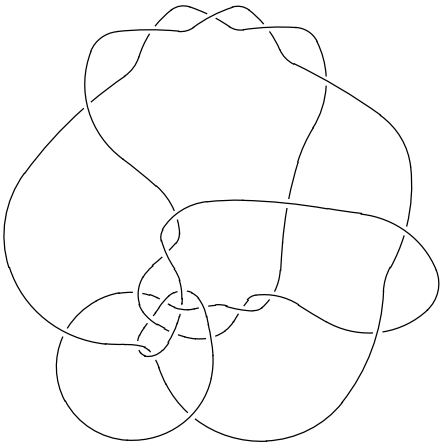

Figure 39. PD[X[14, 11, 15, 1], X[11, 12, 6, 13], X[2, 3, 12, 14], X[13, 5, 4, 15], X[16, 19, 10, 24], X[17, 20, 16, 25], X[20, 17, 26, 18], X[19, 18, 27, 8], X[21, 24, 9, 5], X[22, 25, 21, 6], X[26, 22, 3, 23], X[27, 23, 2, 7], X[39, 40, 7, 1], X[38, 40, 39, 32], X[41, 42, 8, 38], X[37, 42, 41, 36], X[43, 44, 37, 36], X[34, 35, 44, 43], X[33, 31, 35, 34], X[28, 30, 33, 32], X[45, 46, 31, 30], X[29, 10, 46, 45], X[48, 29, 28, 47], X[9, 48, 47, 4]]

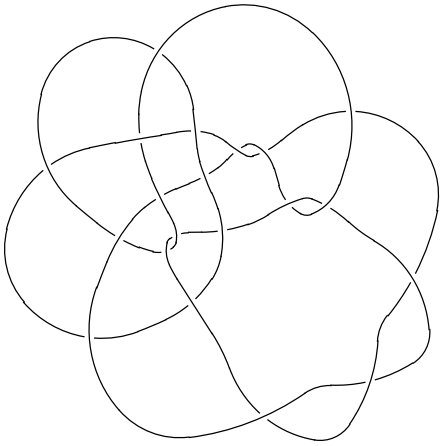

Figure 40. PD[X[11, 8, 12, 38], X[8, 9, 5, 10], X[1, 2, 9, 11], X[10, 4, 3, 12], X[13, 16, 7, 21], X[14, 17, 13, 22], X[17, 14, 23, 15], X[16, 15, 24, 39], X[18, 21, 6, 4], X[19, 22, 18, 5], X[23, 19, 2, 20], X[24, 20, 1, 40], X[32, 33, 39, 40], X[30, 31, 33, 32], X[29, 28, 31, 30], X[25, 27, 29, 38], X[34, 35, 28, 27], X[26, 7, 35, 34], X[37, 26, 25, 36], X[6, 37, 36, 3]]

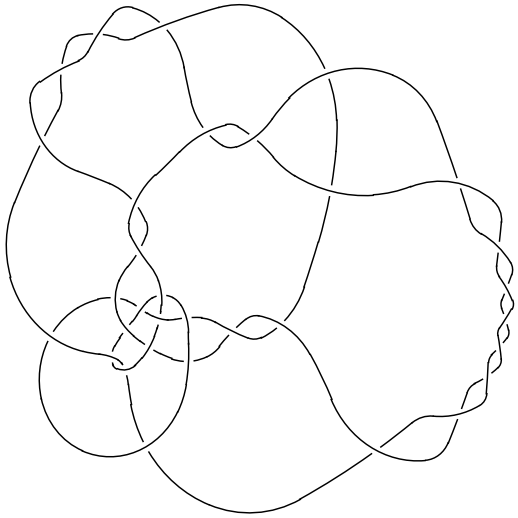

Figure 41. PD[X[14, 11, 15, 1], X[11, 12, 6, 13], X[2, 3, 12, 14], X[13, 5, 4, 15], X[16, 19, 10, 24], X[17, 20, 16, 25], X[20, 17, 26, 18], X[19, 18, 27, 8], X[21, 24, 9, 5], X[22, 25, 21, 6], X[26, 22, 3, 23], X[27, 23, 2, 7], X[49, 50, 7, 1], X[48, 50, 49, 44], X[51, 52, 8, 48], X[47, 52, 51, 46], X[53, 54, 47, 46], X[45, 43, 54, 53], X[55, 56, 45, 44], X[40, 42, 56, 55], X[41, 39, 43, 42], X[28, 38, 41, 40], X[36, 37, 39, 38], X[57, 58, 37, 36], X[34, 35, 58, 57], X[33, 35, 34, 32], X[59, 60, 33, 32], X[30, 31, 60, 59], X[62, 31, 30, 61], X[10, 62, 61, 29], X[64, 29, 28, 63], X[9, 64, 63, 4]]

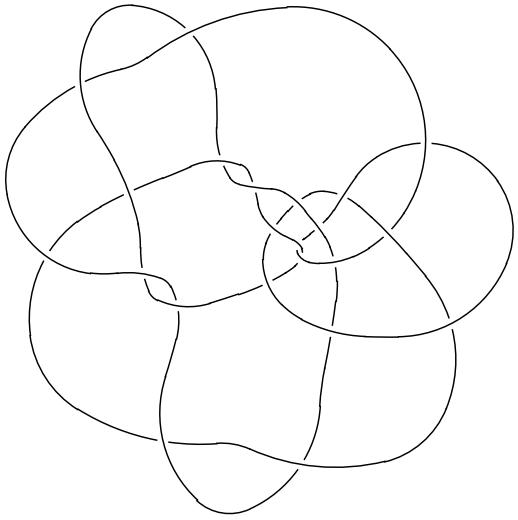

Figure 42. PD[X[10, 7, 11, 40], X[7, 8, 5, 9], X[1, 2, 8, 10], X[9, 4, 3, 11], X[12, 15, 43, 20], X[13, 16, 12, 21], X[16, 13, 22, 14], X[15, 14, 23, 41], X[17, 20, 6, 4], X[18, 21, 17, 5], X[22, 18, 2, 19], X[23, 19, 1, 42], X[34, 35, 41, 42], X[33, 32, 35, 34], X[36, 37, 33, 40], X[29, 31, 37, 36], X[30, 28, 32, 31], X[24, 27, 30, 29], X[25, 26, 28, 27], X[44, 43, 26, 25], X[39, 44, 24, 38], X[6, 39, 38, 3]]

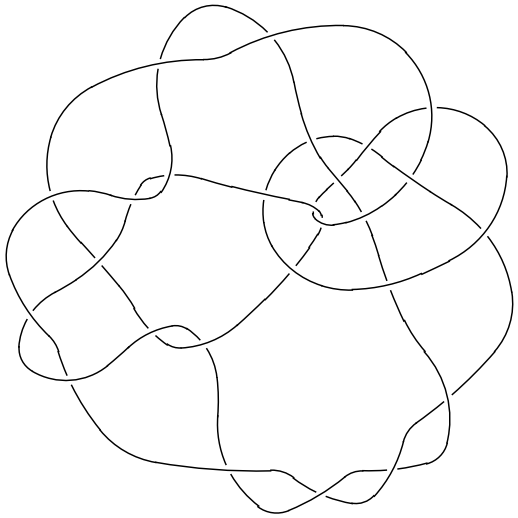

Figure 43. PD[X[14, 11, 15, 1], X[11, 12, 6, 13], X[2, 3, 12, 14], X[13, 5, 4, 15], X[16, 19, 10, 24], X[17, 20, 16, 25], X[20, 17, 26, 18], X[19, 18, 27, 8], X[21, 24, 9, 5], X[22, 25, 21, 6], X[26, 22, 3, 23], X[27, 23, 2, 7], X[41, 42, 7, 1], X[40, 42, 41, 38], X[43, 44, 8, 40], X[37, 44, 43, 39], X[36, 39, 38, 34], X[33, 37, 36, 35], X[45, 46, 35, 34], X[30, 32, 46, 45], X[47, 48, 33, 32], X[31, 10, 48, 47], X[49, 50, 31, 30], X[28, 29, 50, 49], X[51, 52, 29, 28], X[4, 9, 52, 51]]

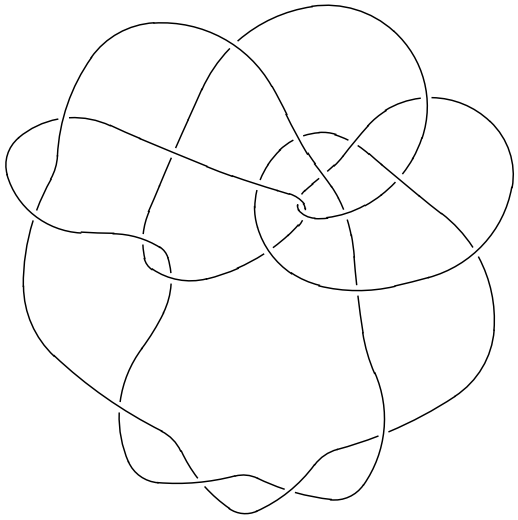

Figure 44. PD[X[11, 8, 12, 42], X[8, 9, 5, 10], X[1, 2, 9, 11], X[10, 4, 3, 12], X[13, 16, 7, 21], X[14, 17, 13, 22], X[17, 14, 23, 15], X[16, 15, 24, 43], X[18, 21, 6, 4], X[19, 22, 18, 5], X[23, 19, 2, 20], X[24, 20, 1, 44], X[33, 44, 42, 31], X[30, 43, 33, 32], X[34, 35, 32, 31], X[27, 29, 35, 34], X[36, 37, 30, 29], X[28, 7, 37, 36], X[38, 39, 28, 27], X[25, 26, 39, 38], X[40, 41, 26, 25], X[3, 6, 41, 40]]

REFERENCES CITED

[1] Susan M. Abernathy. On Krebes's tangle. *Topology Appl.*, 160(12):1379–1383, 2013.

[2] David Eisenbud. *Commutative algebra*, volume 150 of *Graduate Texts in Mathematics*. Springer-Verlag, New York, 1995. With a view toward algebraic geometry.

[3] Victor Guillemin and Alan Pollack. *Differential topology*. AMS Chelsea Publishing, Providence, RI, 2010. Reprint of the 1974 original.

[4] Allen Hatcher. *Algebraic topology*. Cambridge University Press, Cambridge, 2002.

[5] Louis H. Kauffman. State models and the Jones polynomial. *Topology*, 26(3):395–407, 1987.

[6] Louis H. Kauffman. Knot diagrammatics, 2004.

[7] David A. Krebes. An obstruction to embedding 4-tangles in links. *J. Knot Theory Ramifications*, 8(3):321–352, 1999.

[8] W. B. Raymond Lickorish. *An introduction to knot theory*, volume 175 of *Graduate Texts in Mathematics*. Springer-Verlag, New York, 1997.

[9] MANY. The knot atlas.

[10] Tomotada Ohtsuki. *Quantum invariants*, volume 29 of *Series on Knots and Everything*. World Scientific Publishing Co., Inc., River Edge, NJ, 2002. A study of knots, 3-manifolds, and their sets.

[11] K. Reidemeister. *Knot theory*. BCS Associates, Moscow, Idaho, 1983. Translated from the German by Leo F. Boron, Charles O. Christenson and Bryan A. Smith.

[12] Dale Rolfsen. *Knots and links*, volume 7 of *Mathematics Lecture Series*. Publish or Perish, Inc., Houston, TX, 1990. Corrected reprint of the 1976 original.

[13] Morwen B. Thistlethwaite. A spanning tree expansion of the Jones polynomial. *Topology*, 26(3):297–309, 1987.

[14] V. G. Turaev. Operator invariants of tangles, and R-matrices. *Izv. Akad. Nauk SSSR Ser. Mat.*, 53(5):1073–1107, 1135, 1989.

[15] Vladimir Turaev and Alexis Virelizier. *Monoidal categories and topological field theory*, volume 322 of *Progress in Mathematics*. Birkhäuser/Springer, Cham, 2017.